Axion Experiments in Germany 2019

Workshop on Axion Detector Developments in Germany and Around the World

Confirmed Speakers

Dmitry Budker
(CASPER)
Günter Sigl
(Astrophysics)
Dieter Horns
(BRASS)
Nicolò Crescini
(QUAX)

Loredana Gastaldo
(IAXO)
Mikko Mökkönen
(Quantum Detectors)

Libor Šmejkal
(TOORAD)
Frank Steffen
(MADMAX)
Yun Shin
(ARIADNE)
Jan Põld
(ALPS)

Local Organisers

Erik Lentz
David Marsh

Viraf Mehta
Jens Niemeyer

19th - 22nd August

indico.desy.de/event/22889/

Institut für Astrophysik Göttingen

Georg-August-Universität Göttingen

Unterstützt von / Supported by
Alexander von Humboldt Stiftung/Foundation

Outstanding Problems in Axion Cosmology

David J. E. Marsh
CERN, July (2019)

GEORG-AUGUST-UNIVERSITÄT
GÖTTINGEN

Unterstützt von / Supported by

Alexander von Humboldt
Stiftung/Foundation

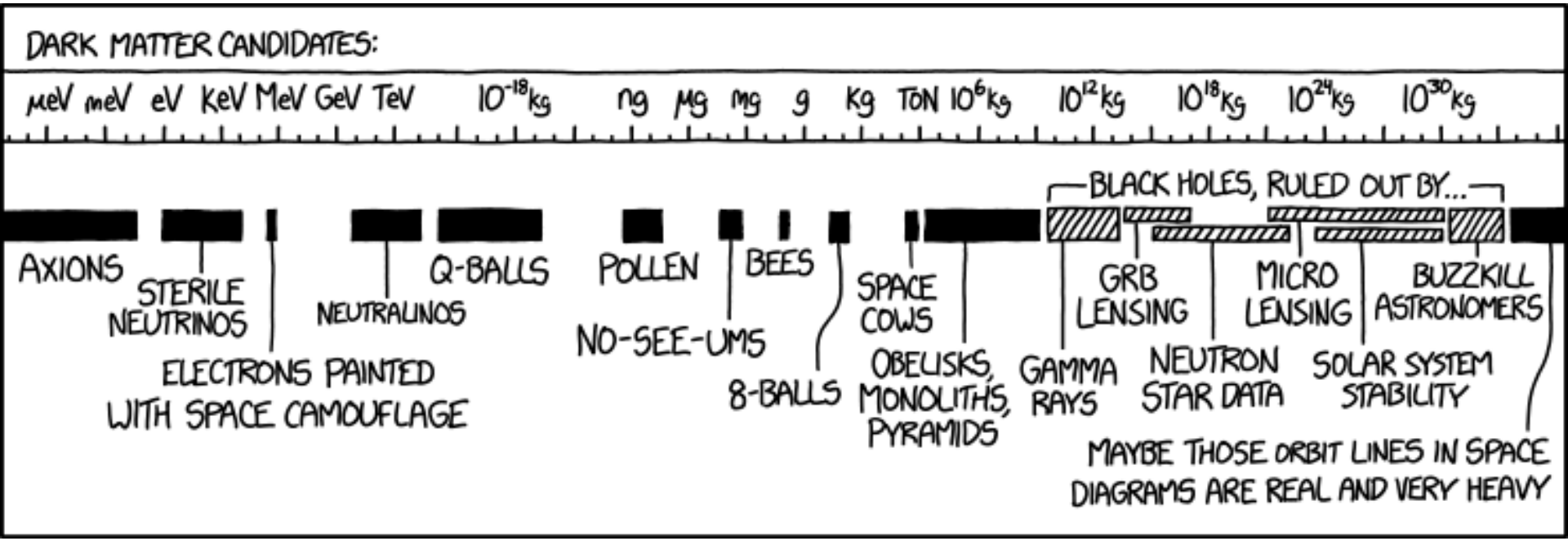

https://xkcd.com/2035/

Ultralight axions:

1. ULAs, the GUT scale, and precision cosmology.
2. Fuzzy DM allowed window.
3. 10^{-15} eV, LISA & the axiverse.

QCD Axion:

1. Relic abundance.
2. Constraints on miniclusters.
3. Detection at high mass.

ULTRALIGHT AXIONS

Fig: Grin, DJEM et al (2019)

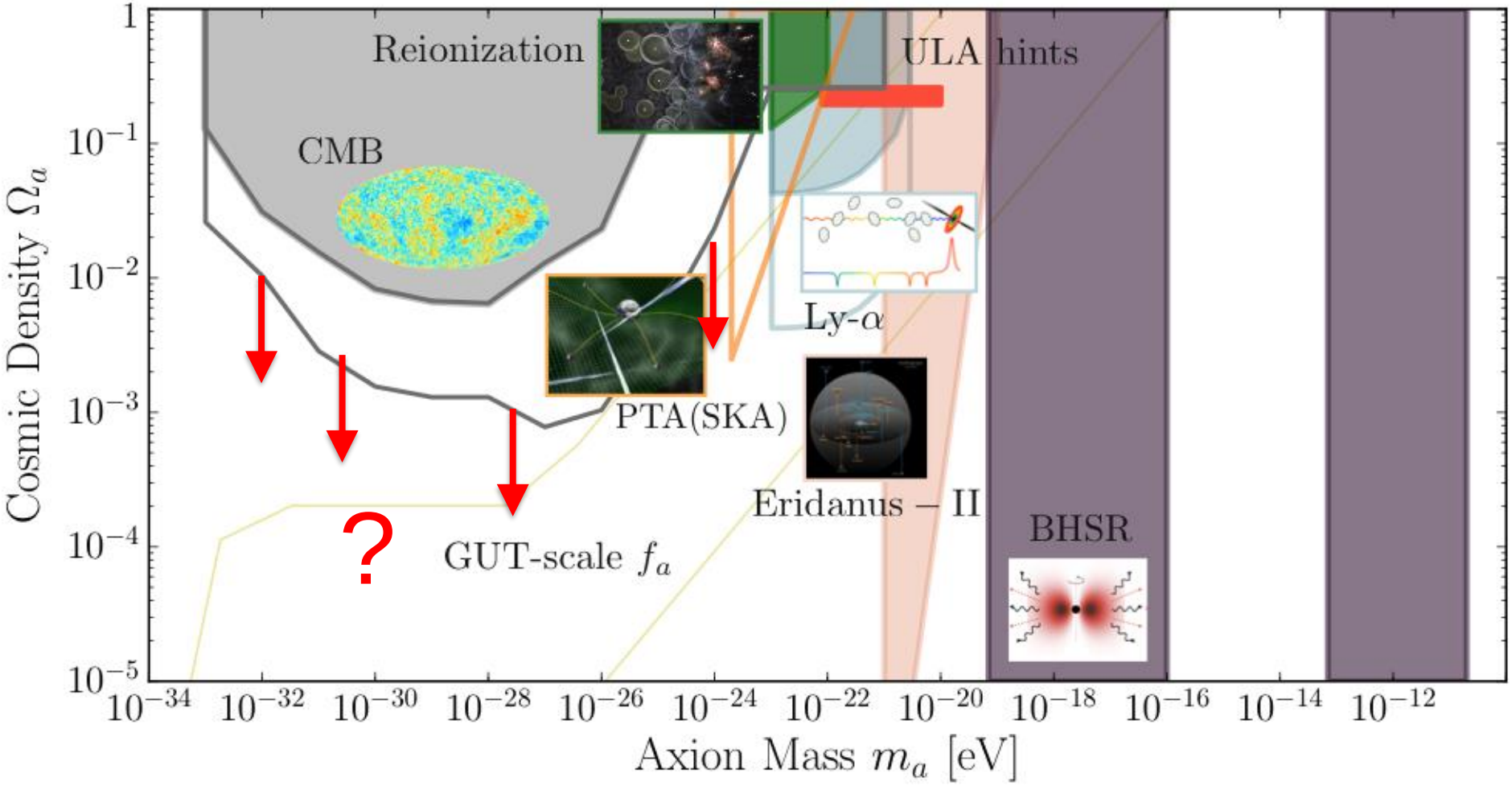

Precision observables beyond CMB-S4: combined probes including 21cm intensity mapping, weak lensing tomography

Two More Regions of Interest

Fuzzy DM allowed region is getting very narrow. Only allowed for:

$$m_a \sim 10^{-21}\ \mathrm{eV}$$

Lower limit: structure formation. Upper limit: Eridanus II heating.

- Is there anywhere left to hide in errors or modelling? OR
- Could we be closing in on the truth? What is a smoking gun?

A second gap exists on the scale of intermediate mass BHs:

$$m_a \sim 10^{-15}\ \mathrm{eV}$$

Acharya et al (2010)

Interestingly, this appears as a prediction of M-theory GUTs.

Could LISA observations shed ~~light~~ GWs on this region?

Fuzzy DM Lower Bound

Assume 100% DM. High-z galaxies and Lyman-α forest:

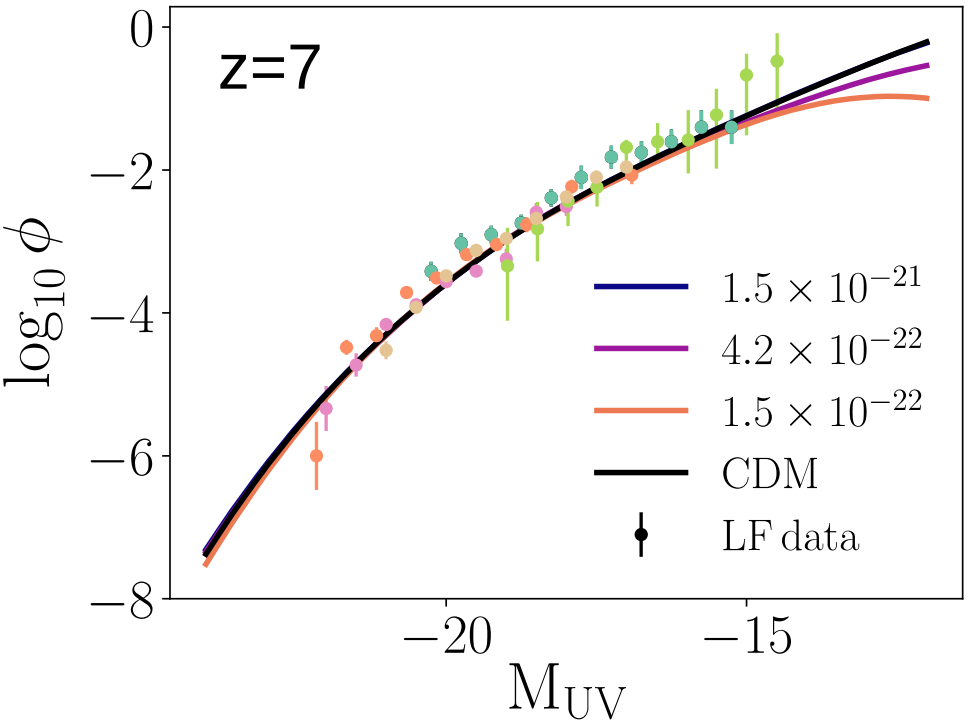

Corasaniti, Agarwal, DJEM, Das (2016)

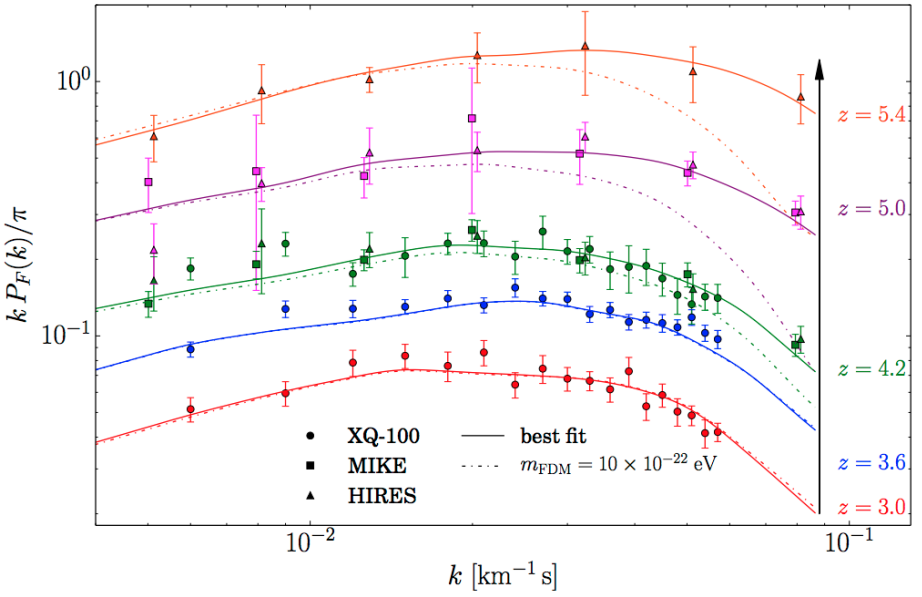

Irsic, Viel, Haehnelt, Bolton & Becker (2017)

Data: Bouwens et al; Atek et al; Livermore et al. z=6,7,8.

Stronger bound, obtained. Baryon parameters fixed → wiggle room with $T_b(x,z)$.

Dynamics in Fuzzy Halos

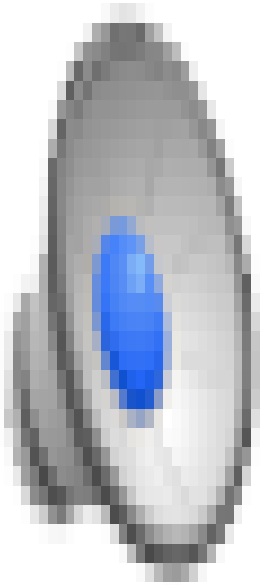

See Tremaine's talk

Veltmaat et al (2018)

Eridanus 2

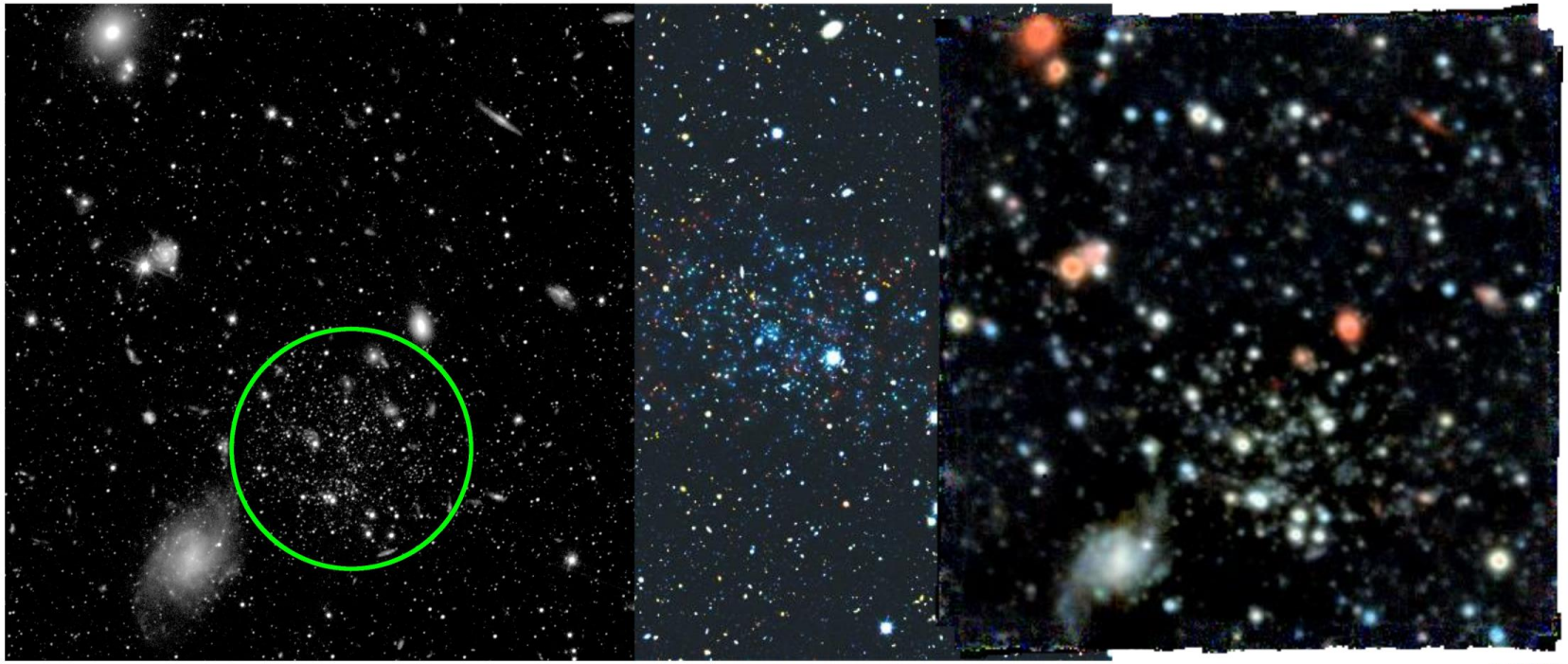

HST (public data, ID 14234, PI J.D. Simon) (image by V. Belokurov & S. Koposov, IoA, Cambridge) MUSE

Eridanus-II

Li et al (2016)

Eri-II is an ultrafaint dwarf galaxy:

$$r_{\rm MW} = 370 \text{ kpc}$$
$$M = 1.2 \times 10^7 \, M_\odot$$
$$\rho_{\rm DM} = 0.15 \, M_\odot \text{ pc}^{-3}$$
$$\sigma_v = 7 \text{ km s}^{-1}$$

with a centrally located star cluster:

$$T = 3 \to 12 \text{ Gyr}$$
$$r_h = 13 \text{ pc}$$
$$M_\star = 2000 \, M_\odot$$
$$\tau_\star \approx 0.1 \text{ Gyr}$$

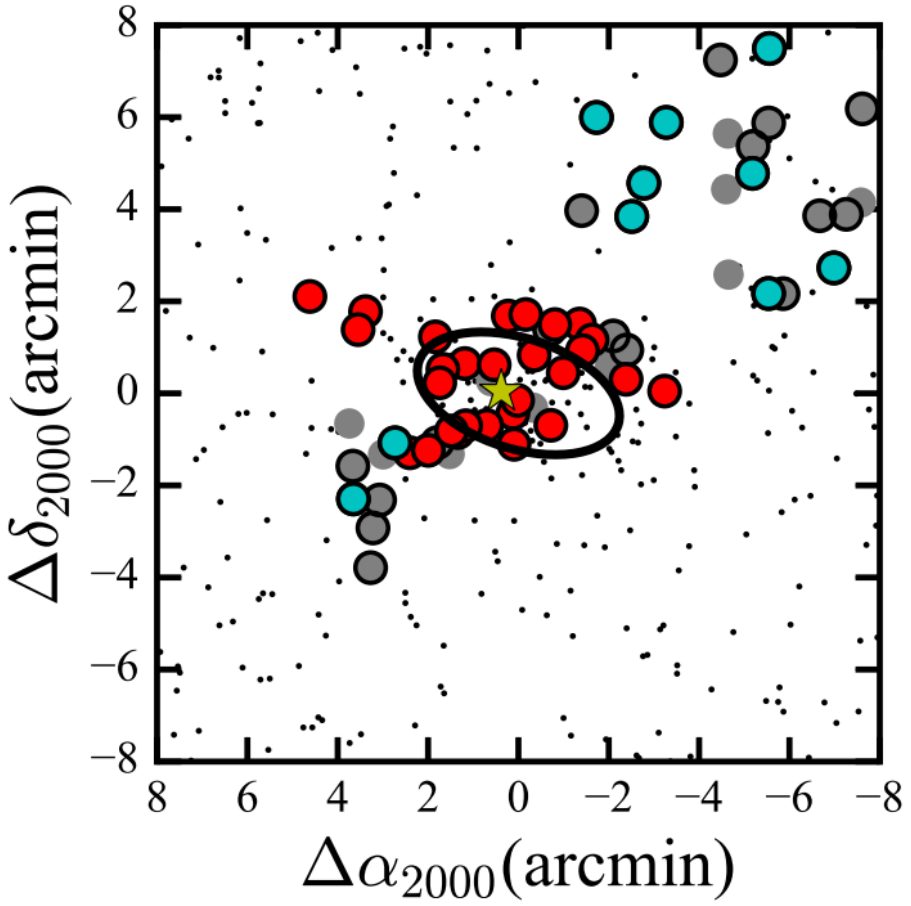

Formation of Eri-II

Niemeyer & DJEM (2018)

Use subhalo-MF of Du et al (2018). Merger trees + stripping.

ıfall mass.

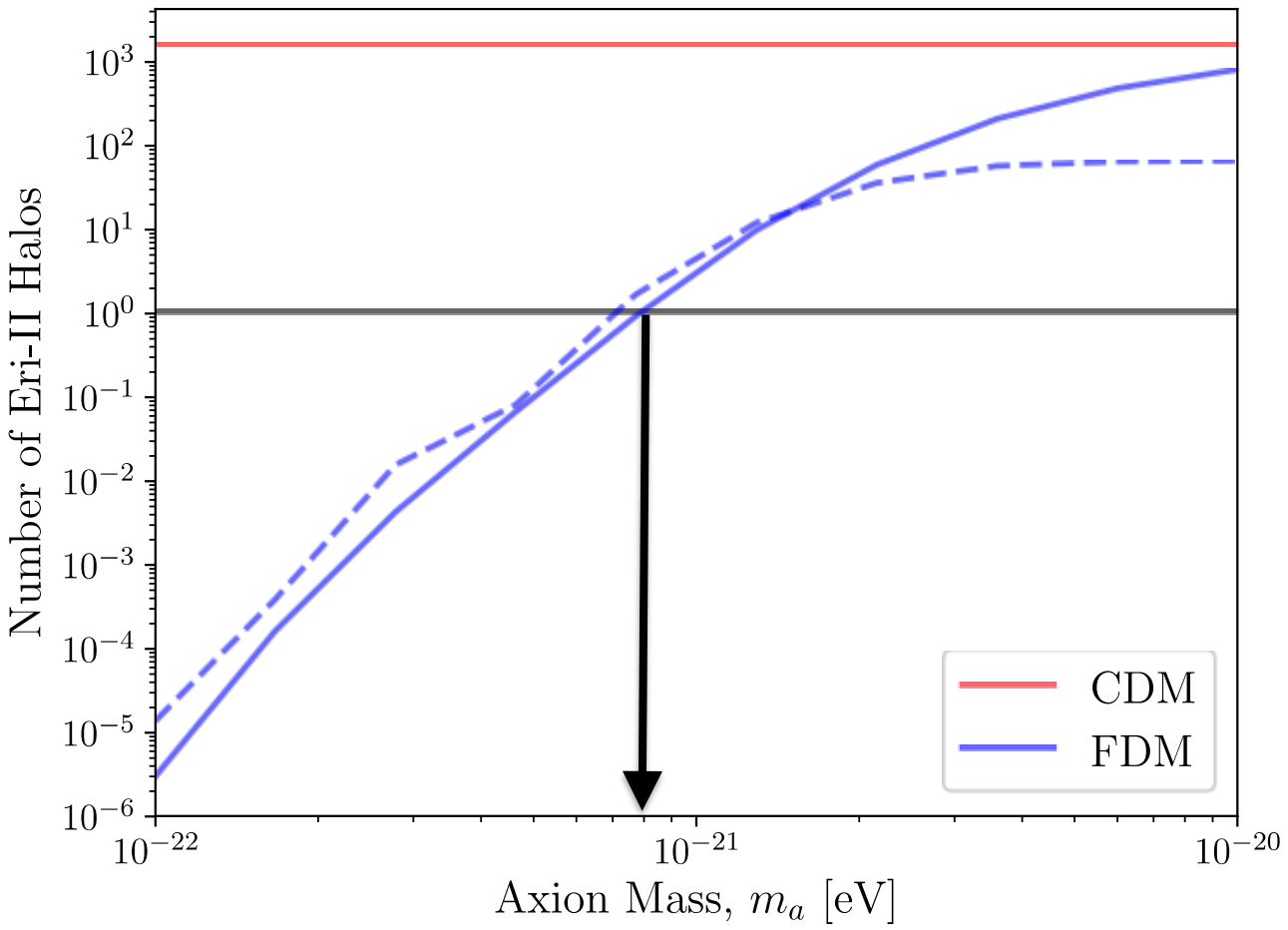

At least one Eri-II mass subhalo in MW →

$$m \gtrsim 0.8 \times 10^{-21}\ \mathrm{eV}$$

The ULA halo has a time-dependent potential with period:

$$\tau_a = \frac{2\pi}{m_a \sigma_v^2} = 0.1 \text{ Gyr} \left(\frac{10^{-21} \text{ eV}}{m_a} \right)$$

In the diffusion approximation, this leads to heating of the star cluster:

$$\frac{dr_h}{dt} = \frac{\Omega_a}{\Omega_d} \frac{8\pi G \rho_0 \mathcal{P}_\delta}{v} \log(k_c v \tau) \left(0.4 \frac{M_*}{\rho r_h^2} + 20 r_h \right)^{-1}$$

Brandt (2016)

In perturbation theory, core oscillations lead to oribtal resonances:

$$\Delta H = 0.3 \frac{\Omega_a}{\Omega_d} \frac{G M_{\rm DM} m}{r} \cos 2\pi t/\tau_a \,,$$

Impose constraints by demanding:

$$r_h(T) - r_h(0) < 13 \text{ pc}$$

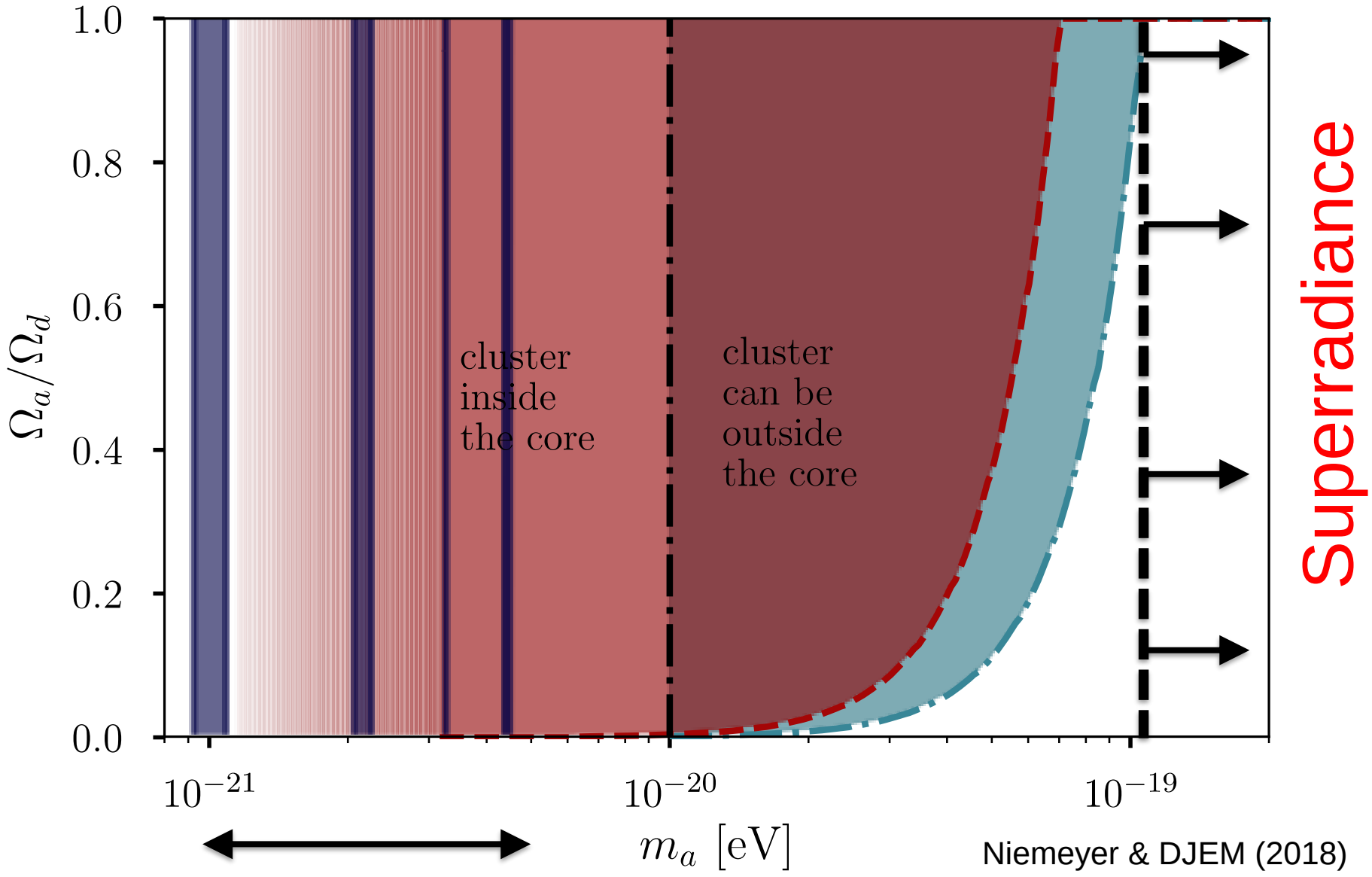

Allowed region between bands and where diffusion breaks down.

→ Resonances predicted in systems with orbital params close

Penrose Process

Fig: Matthew J. Stott

Particle enters Kerr ergoregion, splits in two, one part emerges with more energy than it went in with → spin down BH.

1→2+3

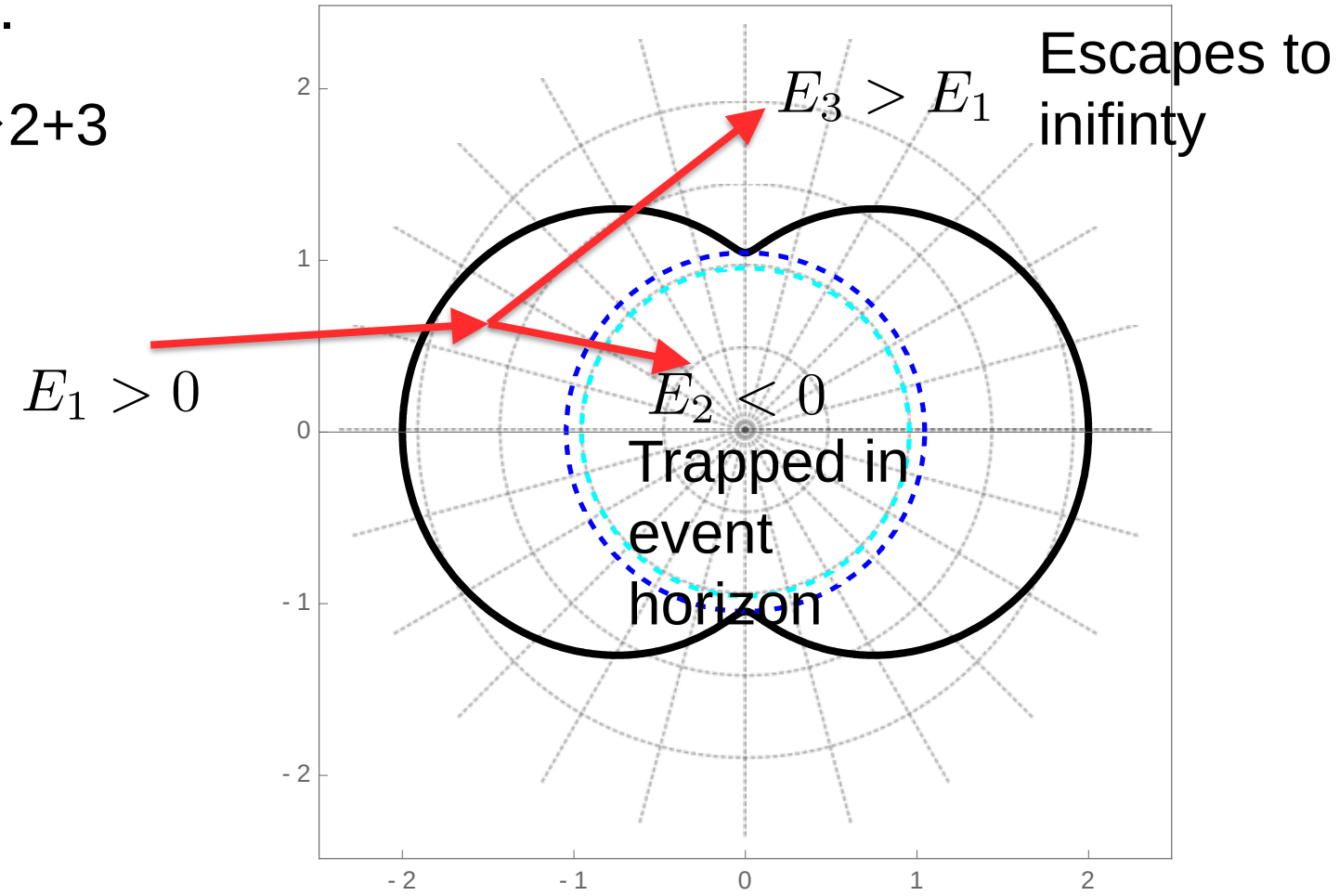

SR: Axion Field on Kerr

$$\Box\phi - \partial_\phi V(\phi) = 0$$

Decompose axion field ϕ into spheroidal harmonics S (c.f. Hydrogen):

$$\phi = \sum_{\ell,m} e^{-i\omega t + im\phi} S_{\ell m}(\theta) R_{\ell m}(r) + \text{h.c.}$$

Angular co-ordinates and quantum number

Eigenvalues ω determine growth/stability. Effective potential, V:

$$\frac{d^2\psi_{lm}}{dr^{*2}} = \left[\omega^2 - V(r,\omega)\right]\psi_{lm}\,.$$

"Tortoise co-ordinate"

Potential as "Mirror"

See Baryakhtar's talk

Arvanitaki & Dubovsky (2010)

A massive boson on Kerr has a "mirror" from its own mass.

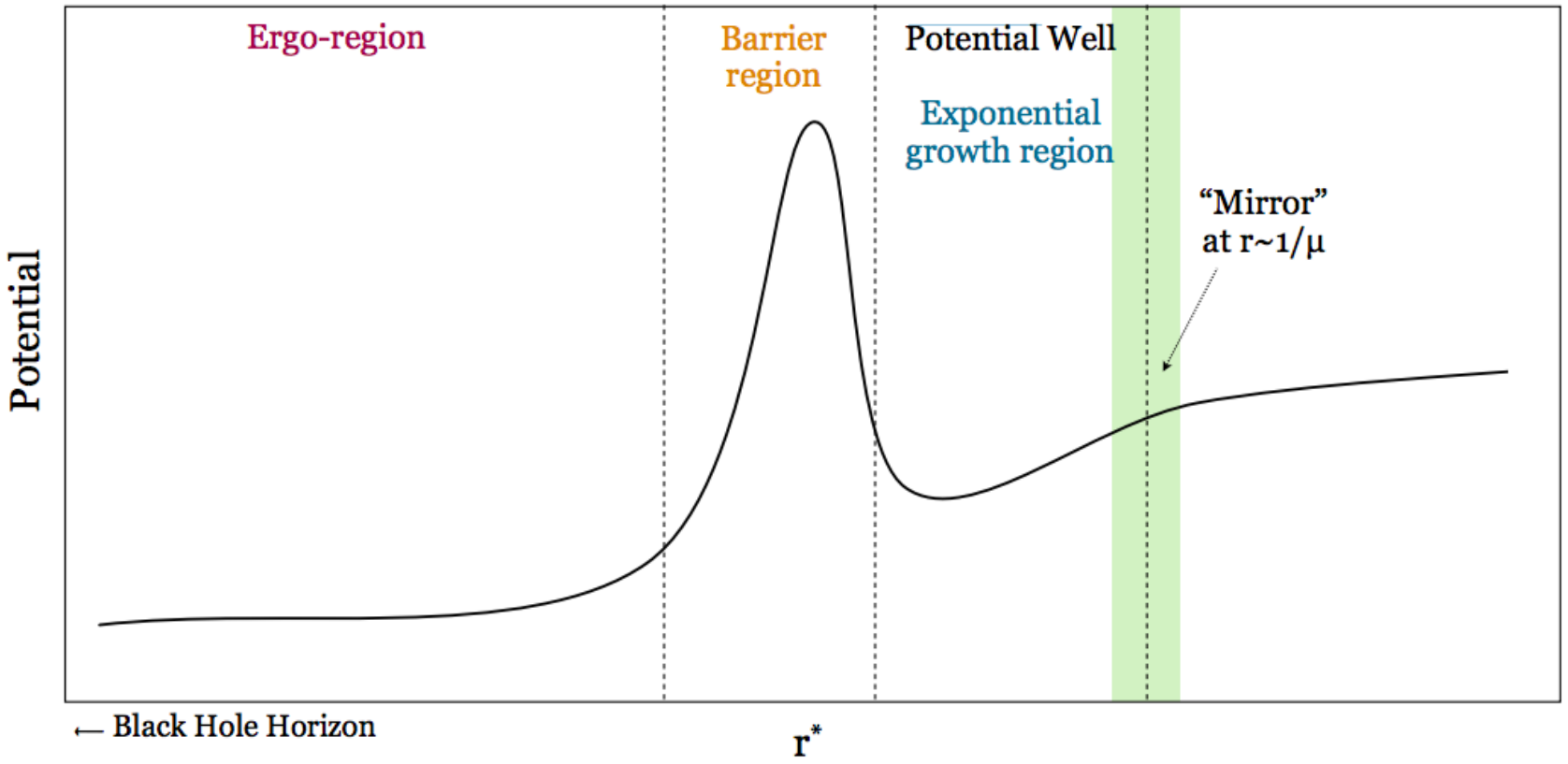

$$V = \frac{4r_g r a m\omega - a^2m^2}{(r^2+a^2)^2} + \frac{\Delta}{(r^2+a^2)}\left(m_a + \frac{l(l+1)+(m_a+\omega^2)a^2}{r^2+a^2} + \frac{3r^2-4r_g r+a^2}{(r^2+a^2)^2} - \frac{3\Delta r^2}{(r^2+a^2)^3}\right).$$

Constraining Axions

BHSR amplifies vacuum fluctations → independent of the axion density.

BHs of certain masses and spins should not be observed if $\tau_{} < \tau$

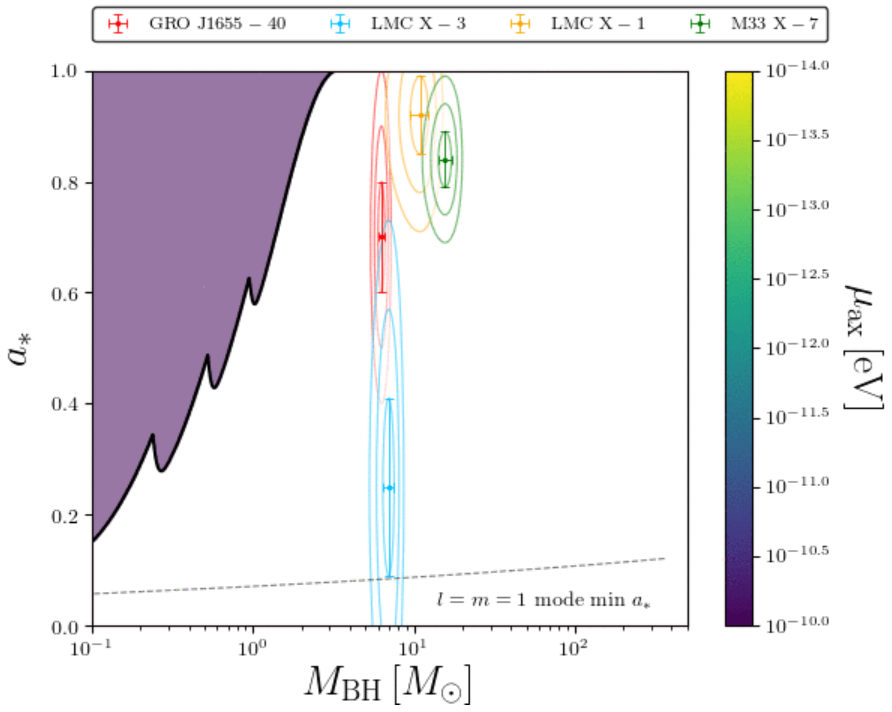

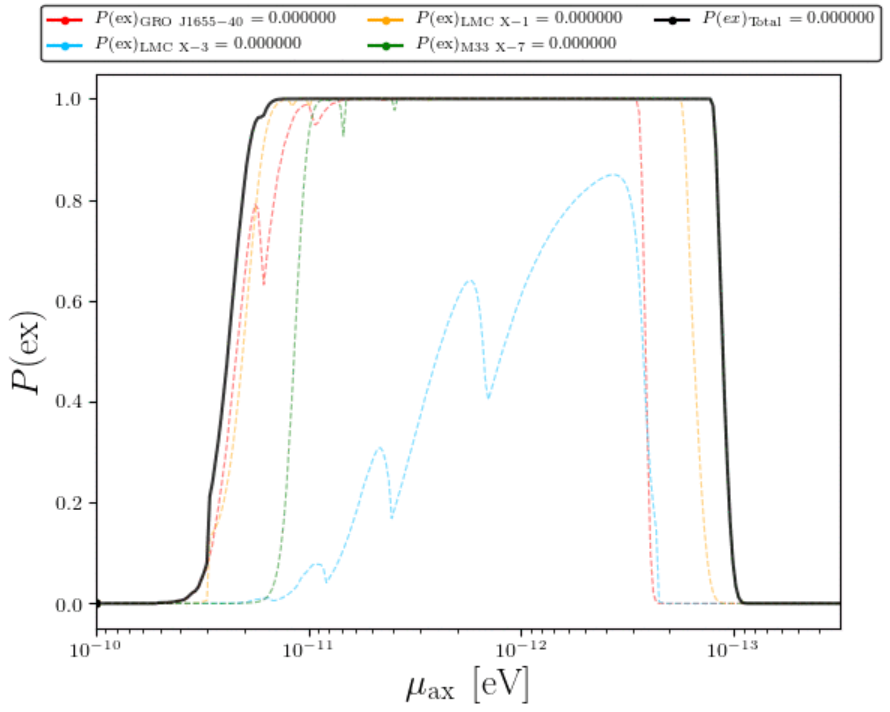

GIF by Matthew J. Stott

Combined Constraints

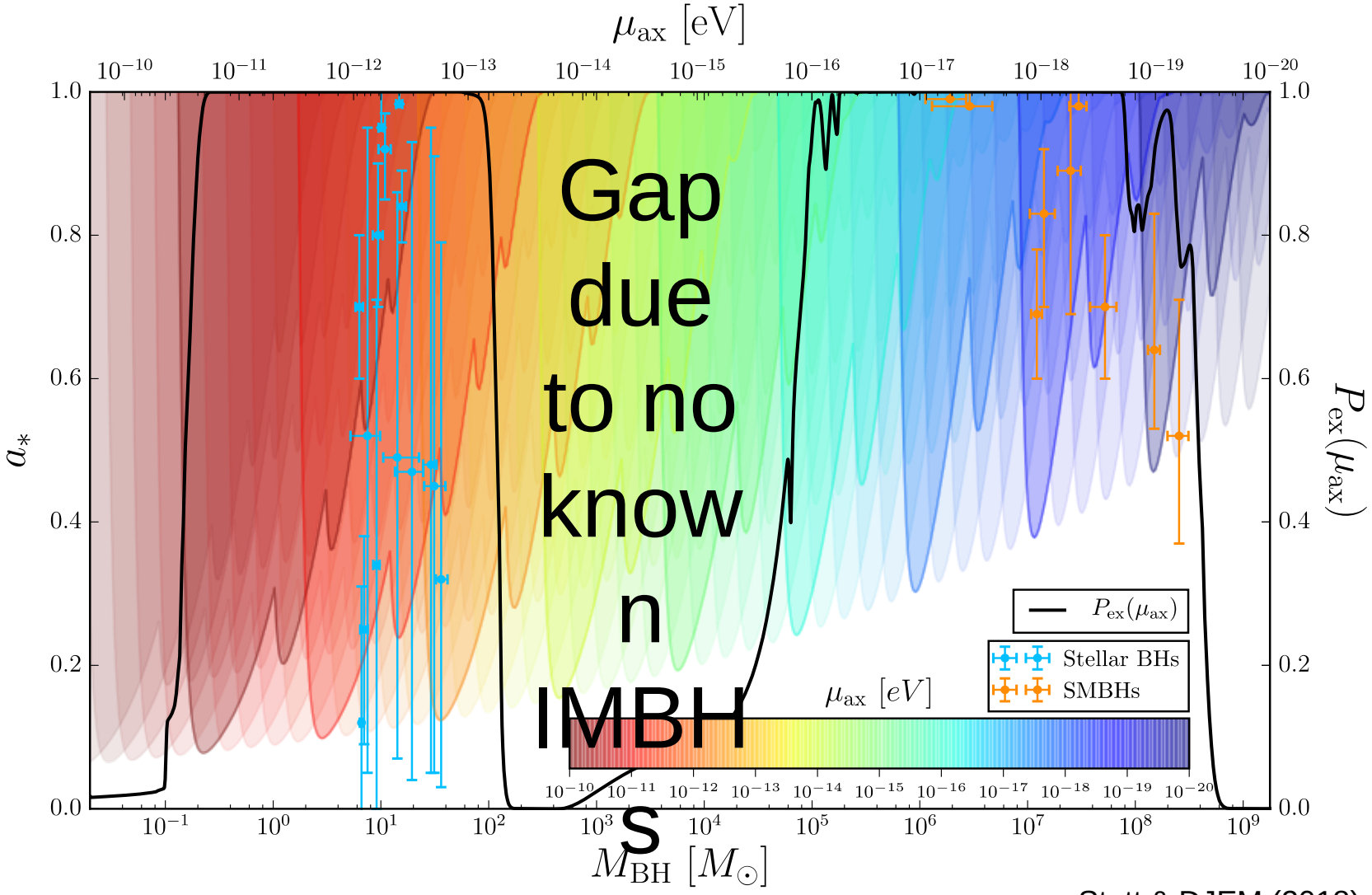

Stott & DJEM (2018)

LISA and IMBHs

Fig: Colpi & Sesana (2016)

IMBH binaries enter LISA band during inspiral.

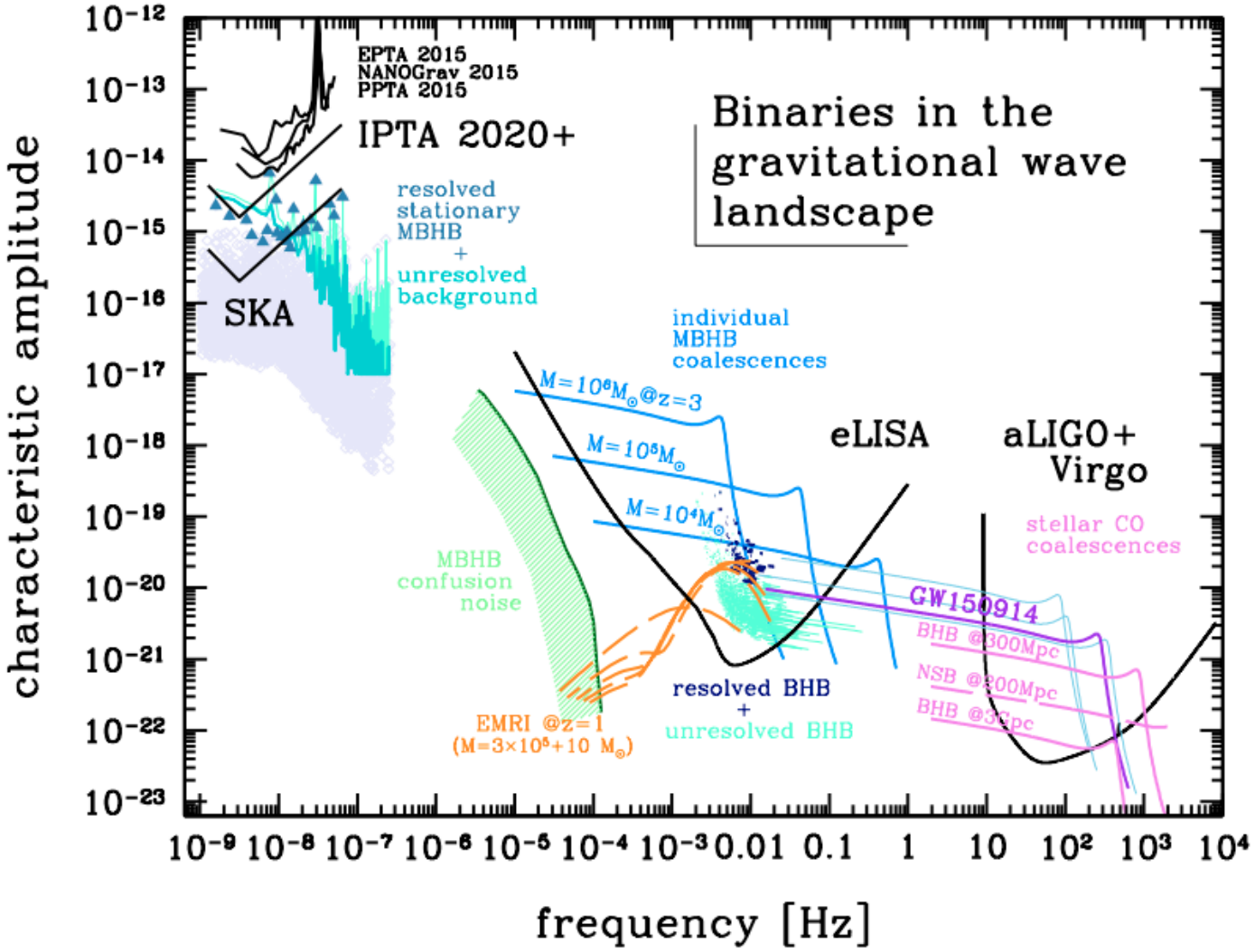

LISA and IMBHs

Brito et al (2017)

IMBH binaries predicted from Pop-III & measurable by LISA.

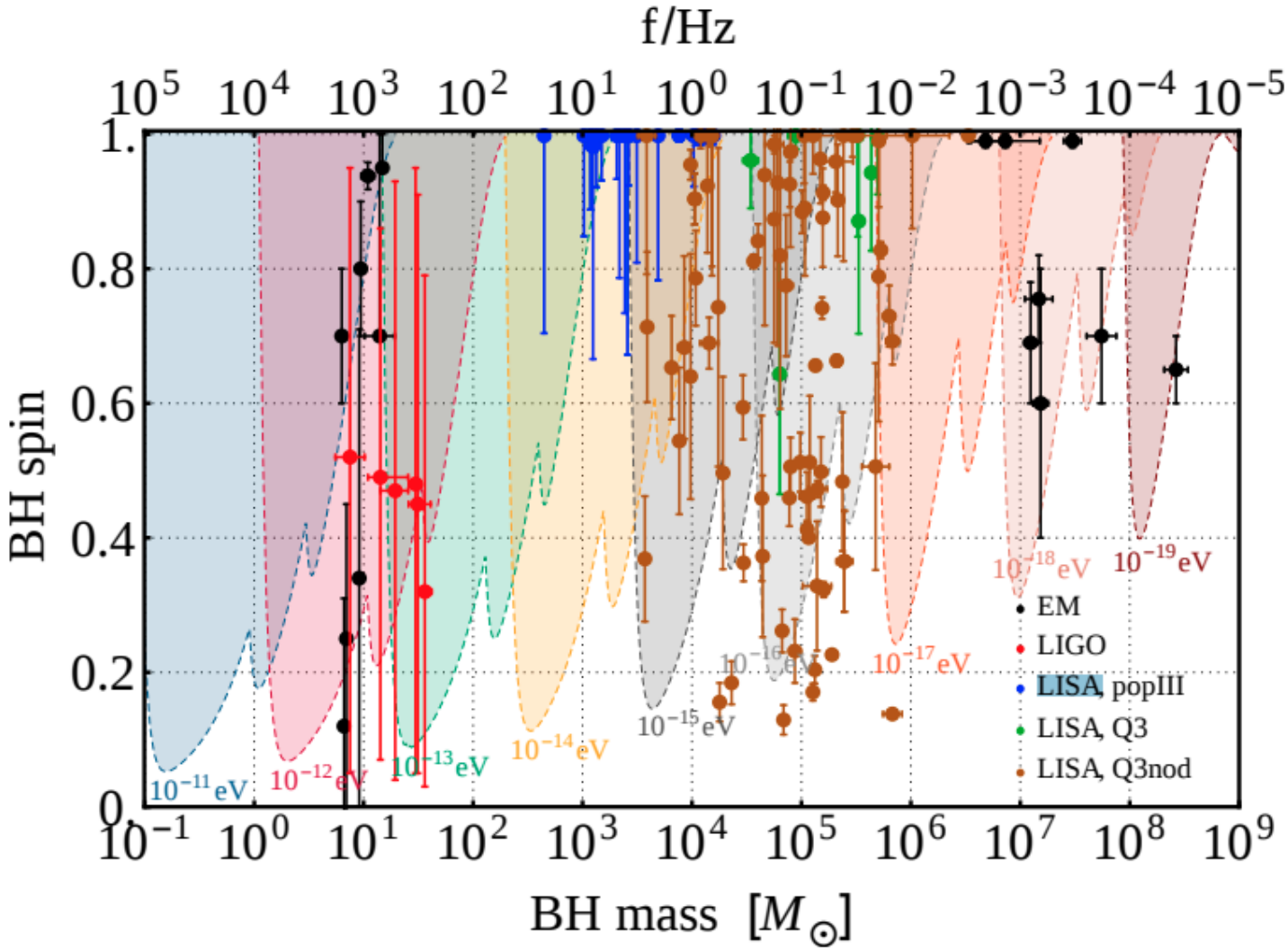

What about the “Axiverse”?

Stott & DJEM (2018)

BHSR can be used to bound the prior distribution of axion

I

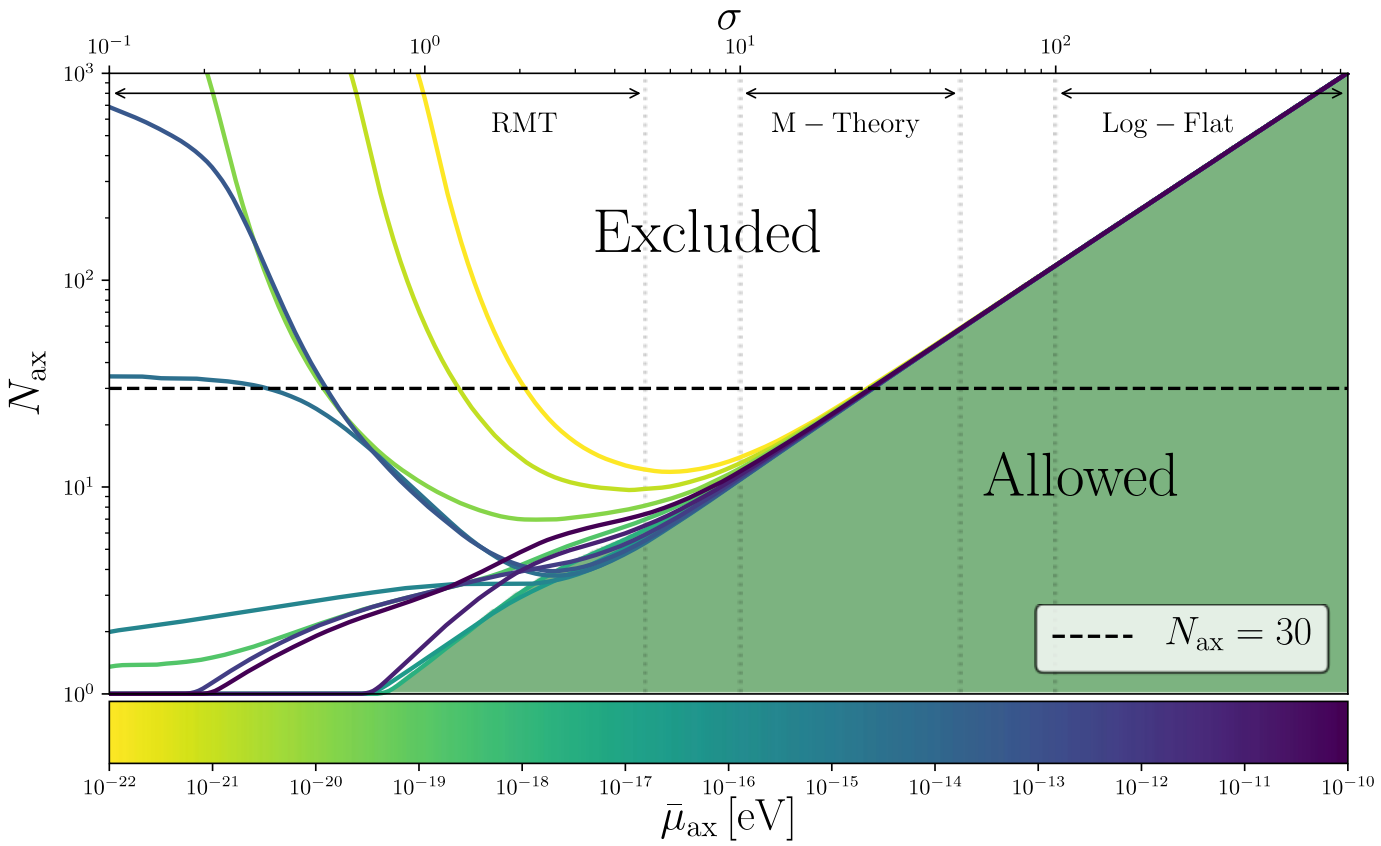

E.g.: log-normal distribution disfavours large numbers of light fields.

Kreuzer-Skarke Axiverse

Demirtas et al (2018)
In prep w/ McAllister et al

Explicit database of Type-IIB CY axiverses up to h^{11}=4

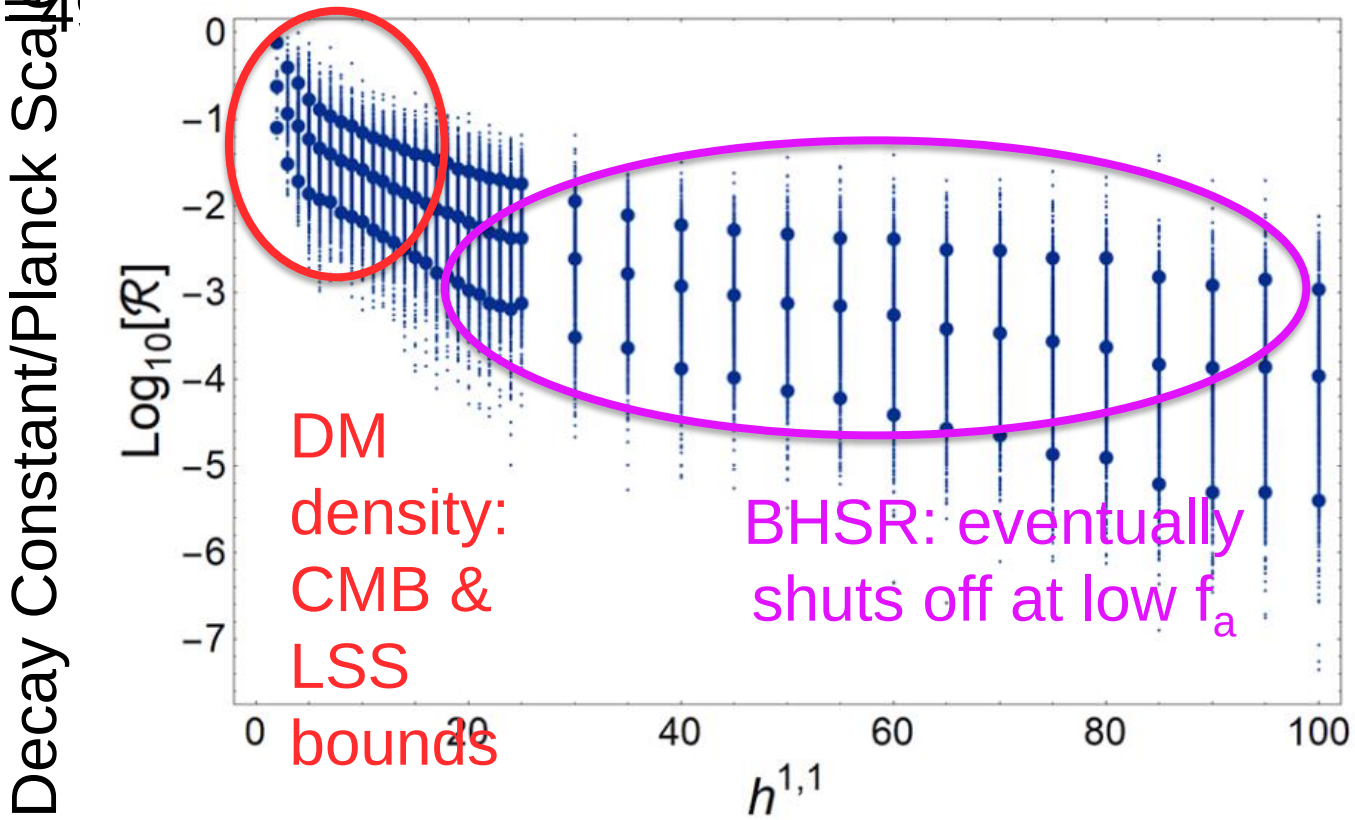

Construct and minimize database potentials → distribution of masses and interaction strengths. Constrain h^{11}?

QCD AXION “CLASSIC” WINDOW

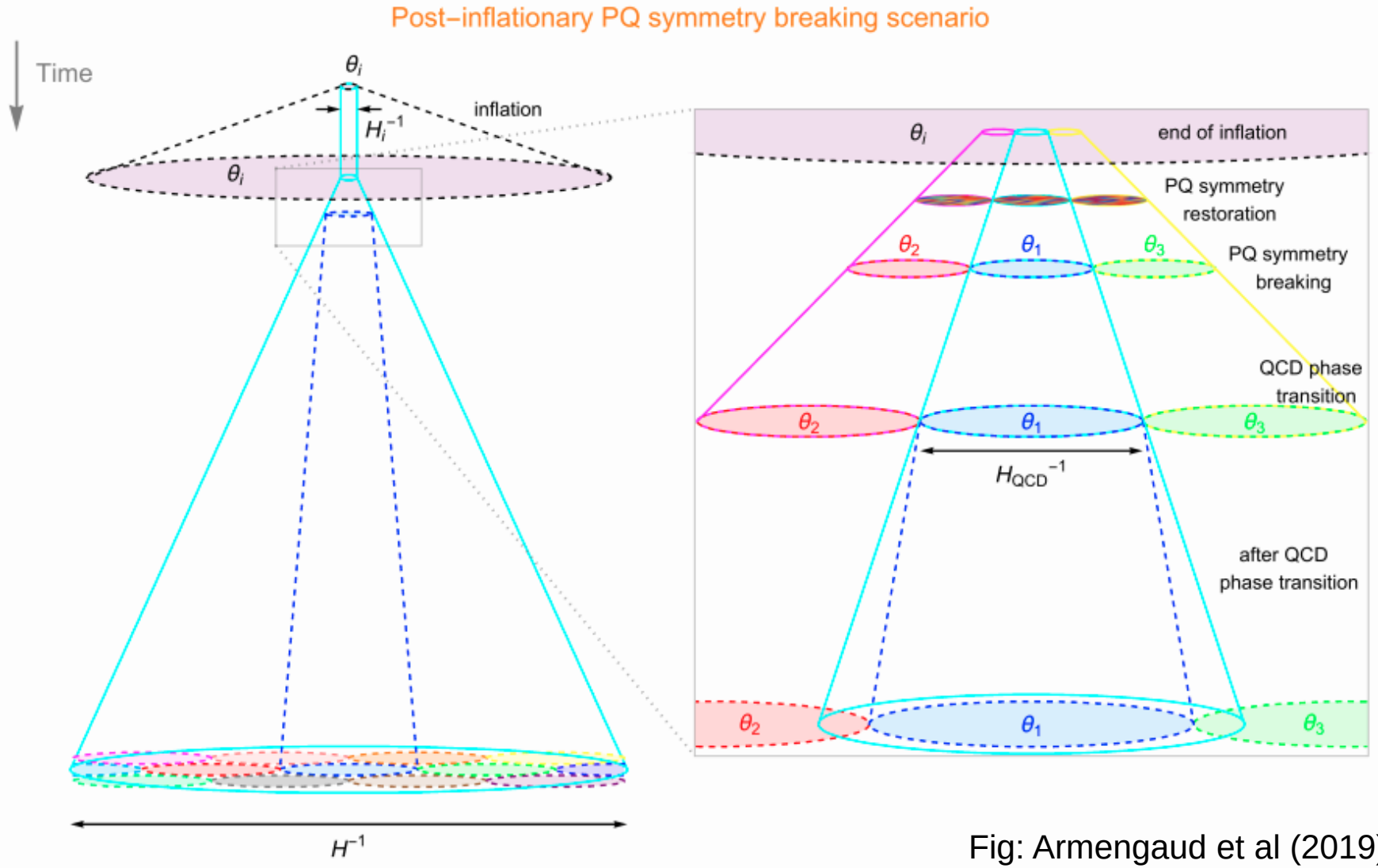

Fig: Armengaud et al (2019)

Large field fluctuations on scales that are sub-horizon today

→ Require (classical) lattice field theory to solve axion

Three Outstanding Problems

1. Relic abundance: this scenario is uniquely predictive. If we can compute the relic abundance we know the axion mass.
2. Miniclusters: dense, gravitationally bound, relics of the phase transition. Can we exclude this scenario using astrophysics, e.g. microlensing?
3. Detection of high mass axions: relic abundance could imply $m>10^{-4}$ eV out of reach of many haloscopes.

These are old problems (1990's), and they are still very hard.

RELIC ABUNDANCE

See Villadoro’s talk and Buschmann discussion

Spontaneous Symmetry Breaking

$H \gg m_\varphi$

$\langle \varphi \rangle = 0$

$\varphi = \chi e^{i\theta}$

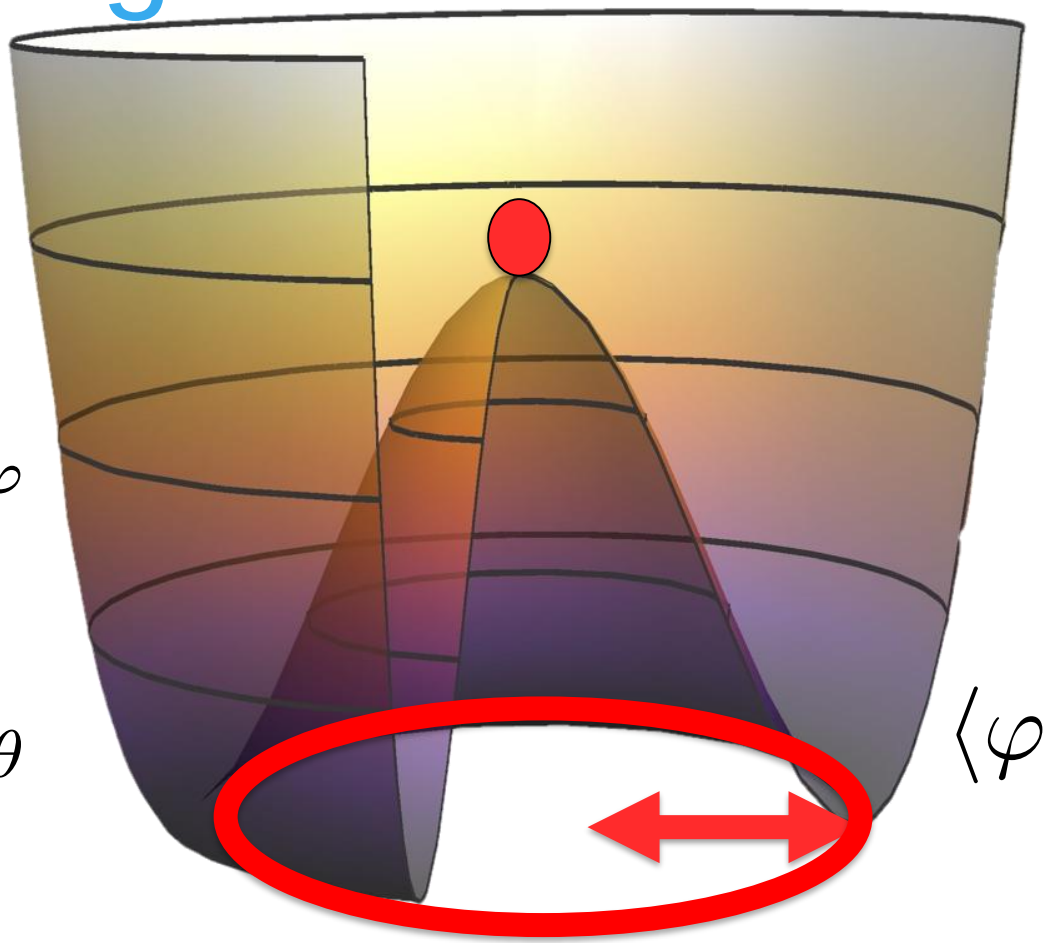

$H \ll m_\varphi$

$\langle \varphi \rangle = f_a/\sqrt{2}$

$\theta = \phi / f_a$

String Formation

Kibble (1976,1980)

SSB leads to a mapping from the complex plane of the field [which has symmetry group U(1)] to the physical space, which has symmetry group R3 → formation of "topological defects":

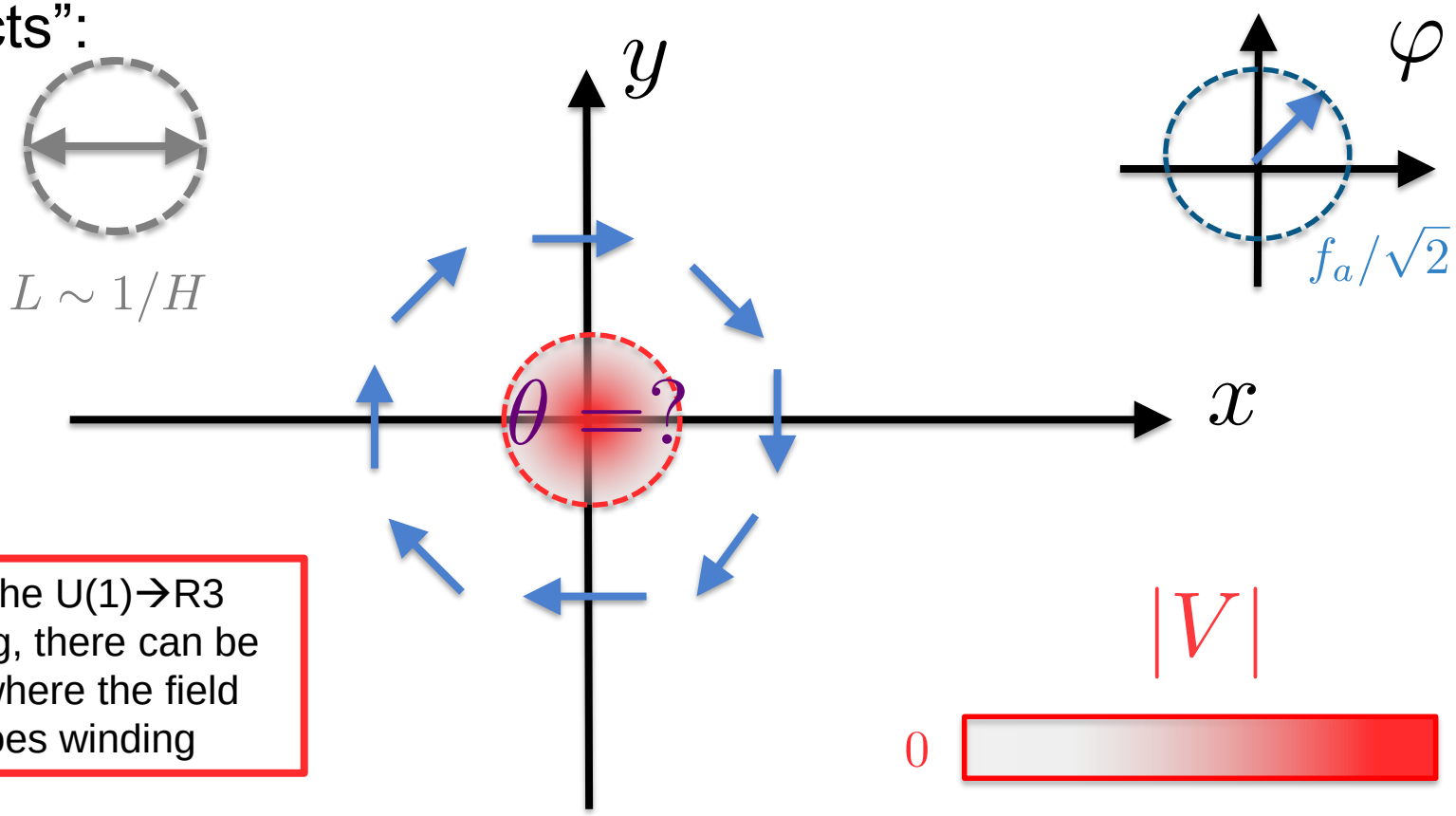

Due to the U(1)→R3 mapping, there can be points where the field undergoes winding

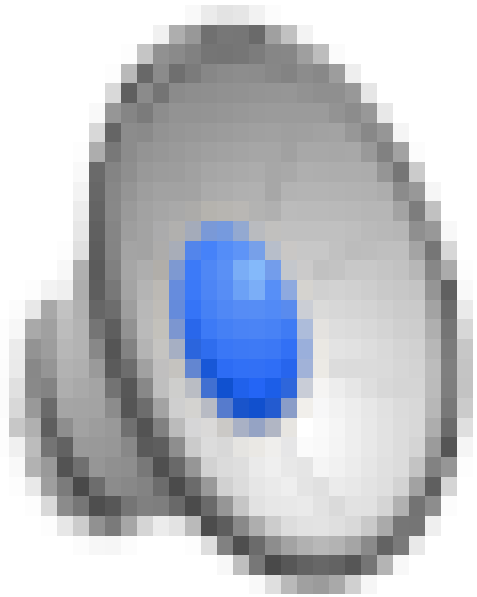

Gorghetto et al (2018)
https://www.youtube.com/watch?v=DbvM7emtodo

Hierarchies Restrict Simulation

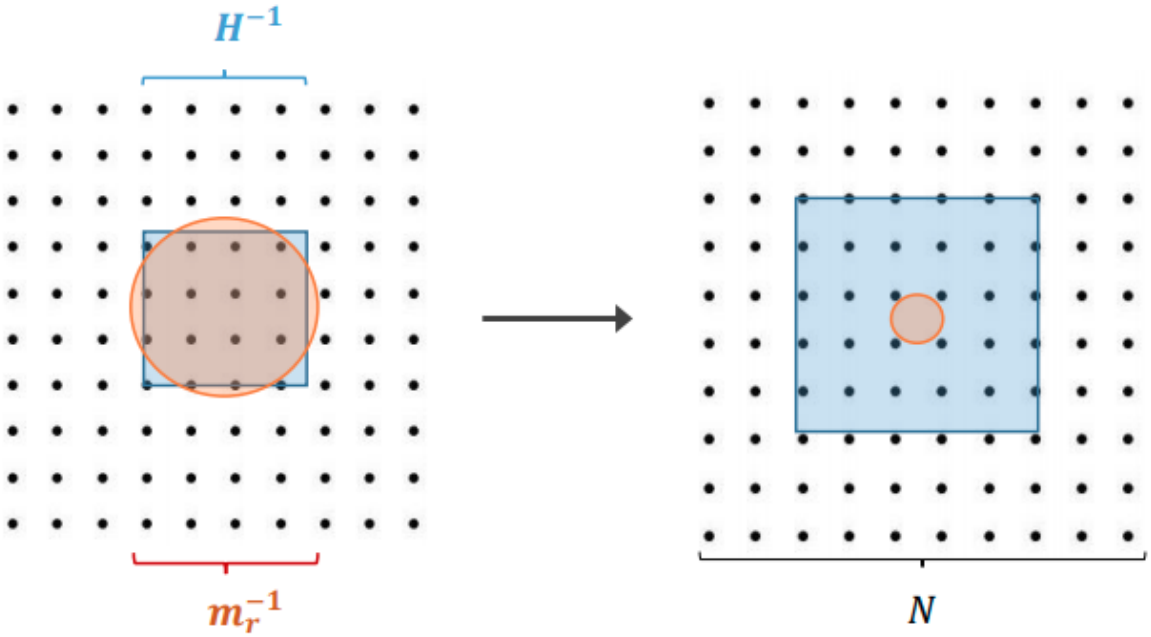

$$\log \frac{m_r}{H} = \log(\frac{\square}{\bigcirc}) \lesssim 6$$

Fig: Gorghetto et al (2018)

1. Small log range and extrapolate.
2. “PRS” or “fat string” approx.
3. Multi-field trick.

Hiramatsu et al, Gorghetto et al

Vaquero et al, Gorghetto et al

Klaer & Moore

See also Buschmann et al

Axions From String Decay

Integrate the string spectrum:

$$n_a(t) = \int \frac{\mathrm{d}k}{k} \frac{\partial \rho}{\partial k}$$

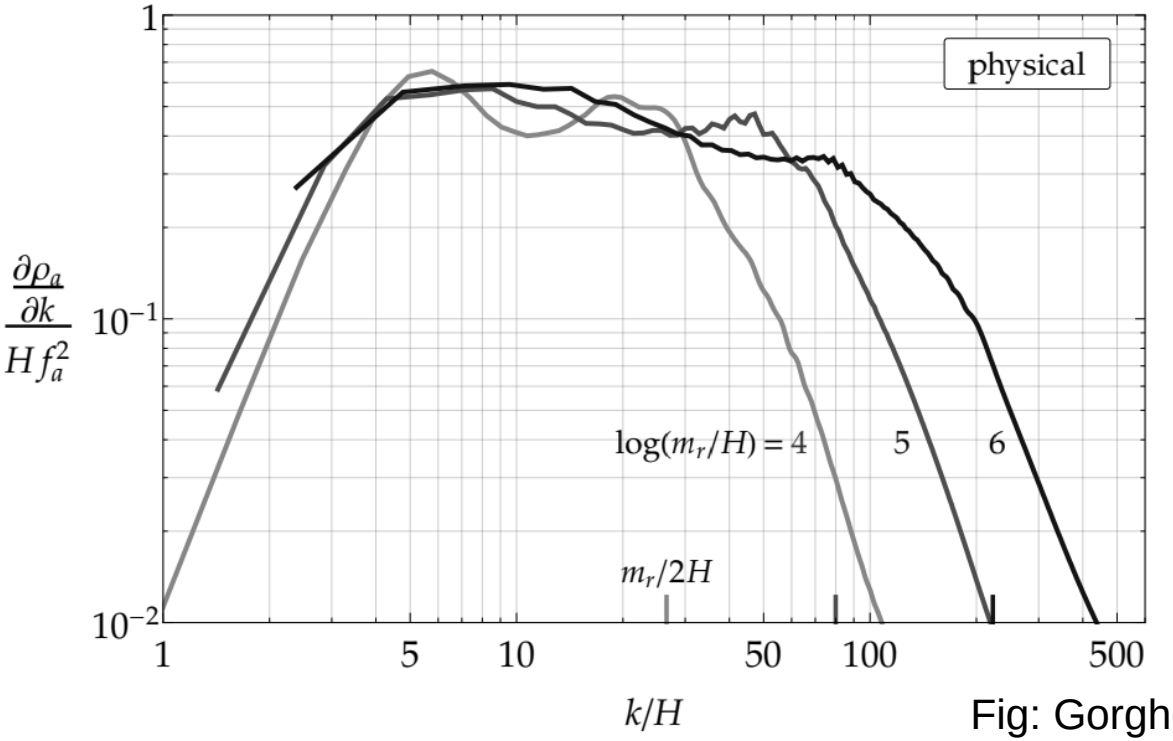

Fig: Gorghetto et al (2018)

Axions From String Decay

Parameterise your ignorance:

1. Compute the “naïve” misalignment result with the average value (many horizon volumes):

$$\langle \theta^2 \mathcal{F}_{\rm an}(\theta) \rangle = \frac{1}{2\pi} \int_{-\pi}^{\pi} {\rm d}\theta \; \theta^2 \mathcal{F}_{\rm an}(\theta) = c_{\rm an.} \frac{\pi^2}{3}$$

2. Introduce an additional fudge factor fit to simulations:

$$\Omega_a h^2 = \Omega_a h^2|_{\rm mis.} (1 + \alpha_{\rm dec.})$$

Computing α: extrapolation

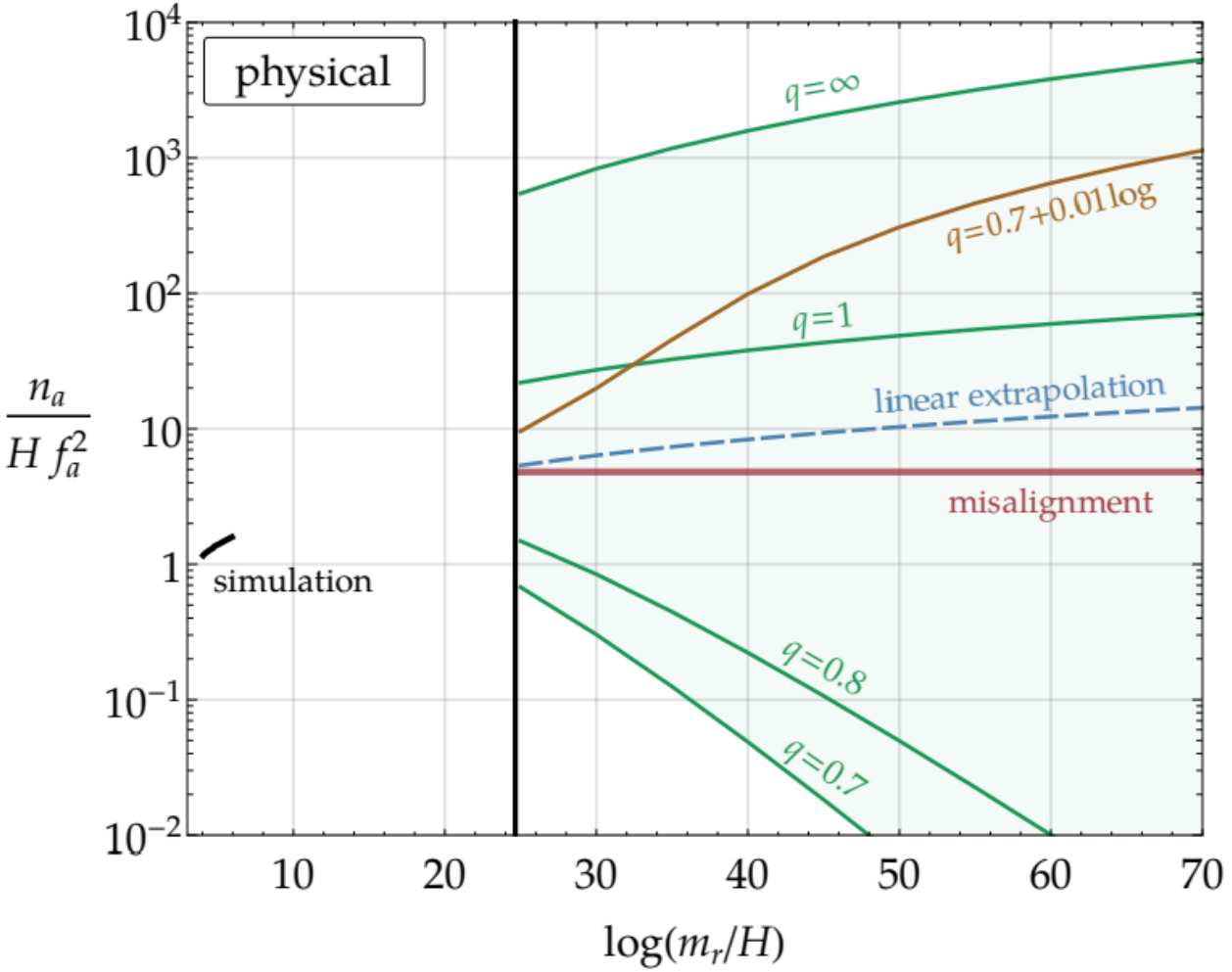

$$\alpha_{\rm dec} \sim 100$$

$$\alpha_{\rm dec} \sim 1$$

$$\alpha_{\rm dec} < 0\ !$$

Gorghetto et al (2018)

Domain Walls

Fig: Armengaud et al (2019)

If the colour anomaly N_{DW}>→ multiple CP-conserving vacua

→ require mechanism for d

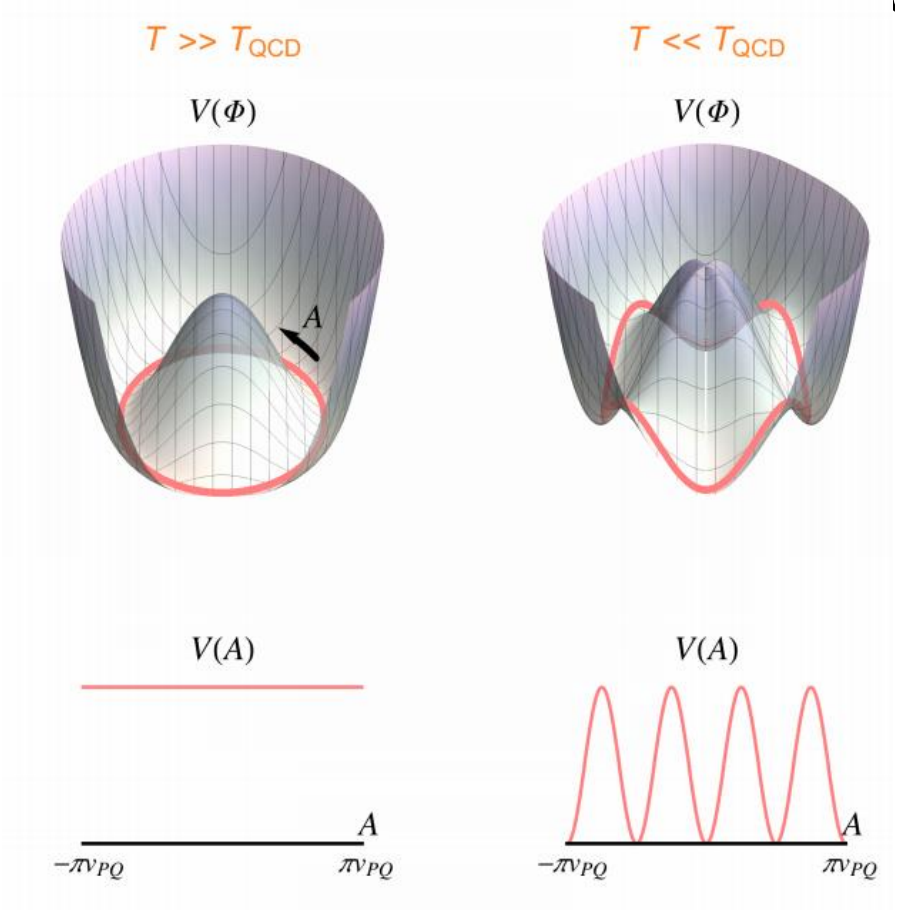

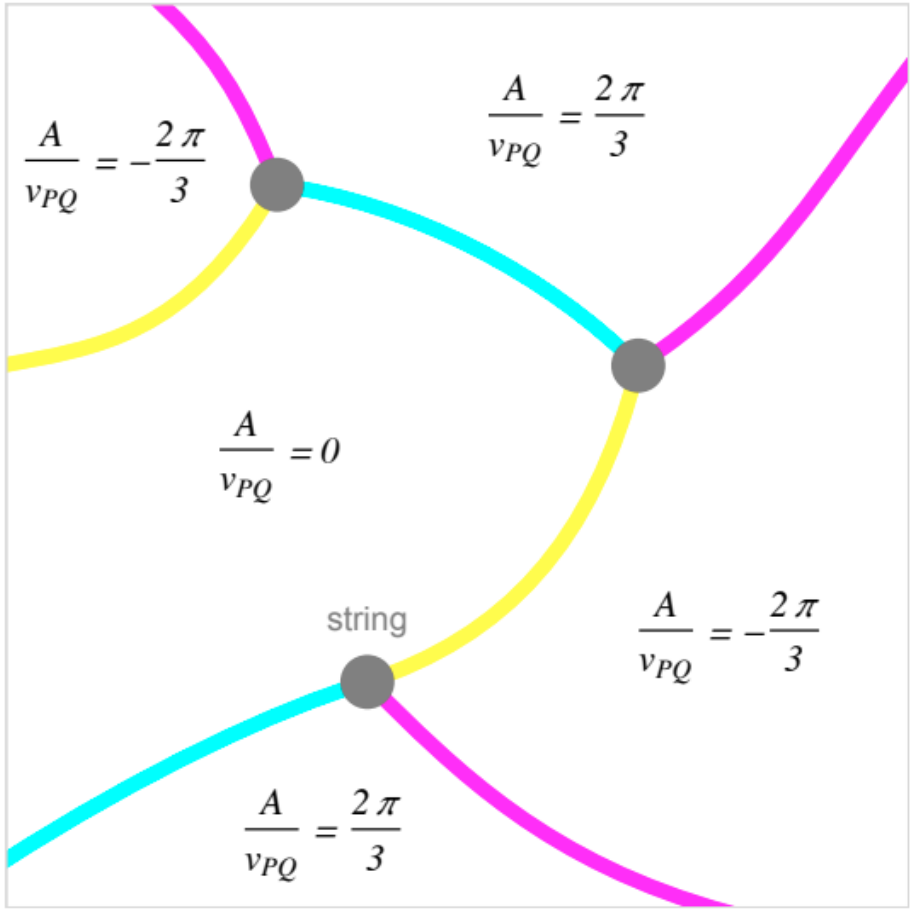

The Axion Mass

Armengaud et al (2019)

Simplest KSVZ-like model (N_{DW}=1) w/ string uncertainties:

$$2.6 \times 10^{-5}\ \mathrm{eV} \lesssim m_a \lesssim 4.4 \times 10^{-3}\ \mathrm{eV}$$

N_{DW}>1 requires explicit PQ breaking. Protect with Z_N symmetry.

Consider DFSZ with N_{DW}=6 and N=10,9:

$$5.8 \times 10^{-4}\ \mathrm{eV} \lesssim m_a \lesssim 4.5 \times 10^{-3}\ \mathrm{eV}$$

$$5.8 \times 10^{-4}\ \mathrm{eV} \lesssim m_a \lesssim 1.3 \times 10^{-1}\ \mathrm{eV}$$

→ a lot of this parameter space is inaccessible to cavity haloscopes.

SEARCHING FOR MINICLUSTERS

Related objects: see Arvanitaki's talk

Miniclusters

Hogan & Rees (1988); Kolb &Tkachev (1993+)

After string decay, axion field has O(1) fluctuations on length scales O(1/H) → isocurvature perturbations → bound structures

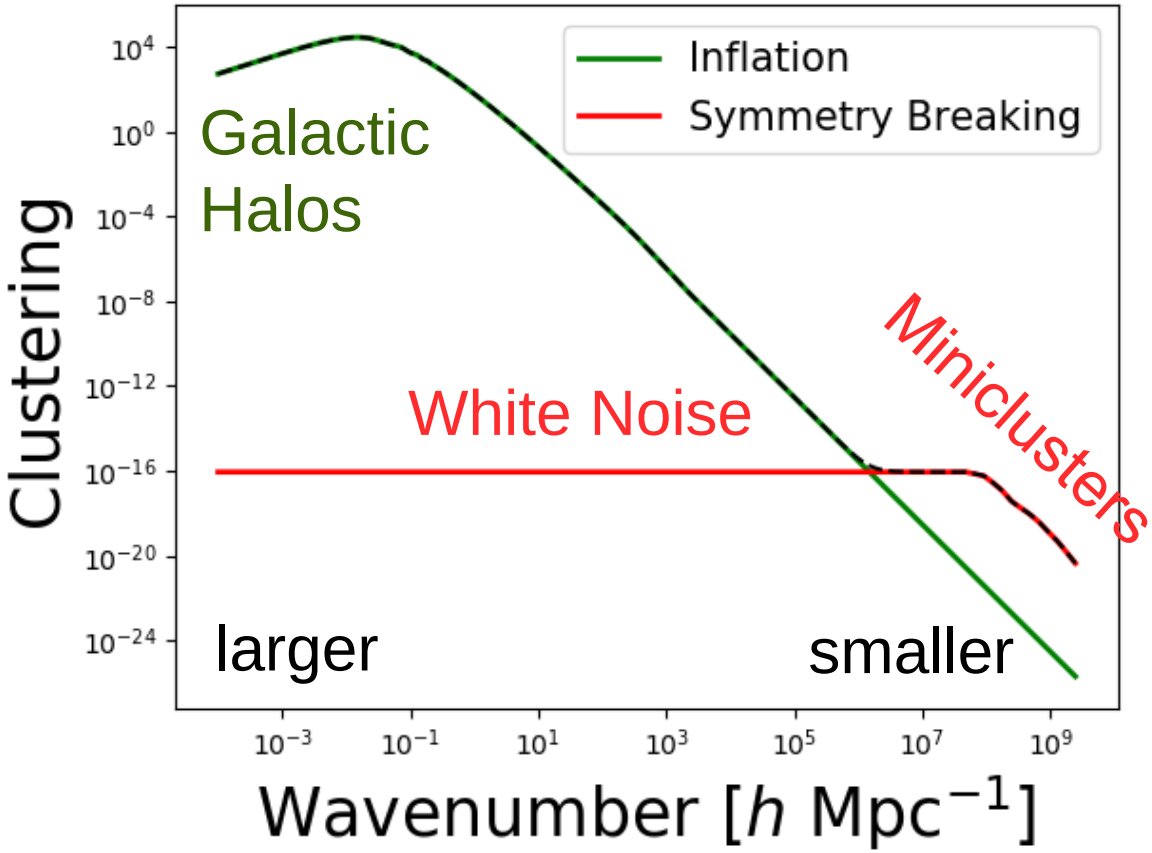

Miniclusters

Large density perturbations on L~1/H(a_{osc}), DM mass in region::

$$M_0 \approx f_{\rm MC}\bar{\rho}_a \left(\frac{a_0}{a_{\rm osc}}\right)^3 \times \frac{4}{3}\pi L_{\rm mc}^3$$

$$L_{\rm mc} \approx \xi^{-1/3}\frac{\pi}{k_{\rm osc}} \sim \xi^{-1/3}\frac{\pi}{H_{\rm osc}}$$

Unknown quantites:

- # of strings → # MCs per horizon, ξ. $\xi = 1 \rightarrow 10$
- Fraction of DM in MCs, fMC. $f_{\rm MC} = 0.5 \rightarrow 1$

Minicluster Mass

Consider generic ALP, with ma,fa and m(T) free. Fix fa by $\Omega_a h^2$:

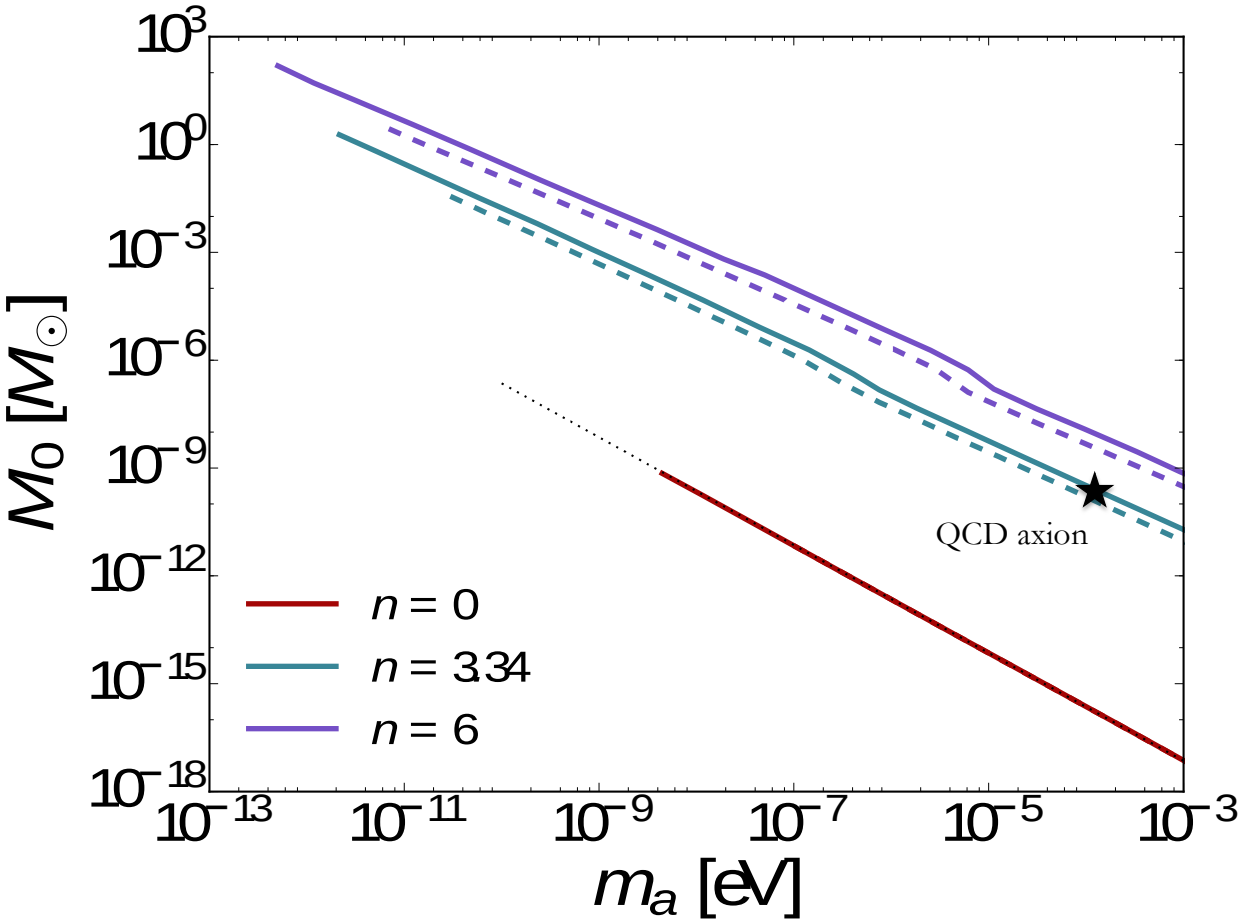

QCD axion: $M_0 \approx 10^{-10} M_\odot$ if ξ=1, fMC = 1.

Initial conditions from field theory on lattice without gravity.

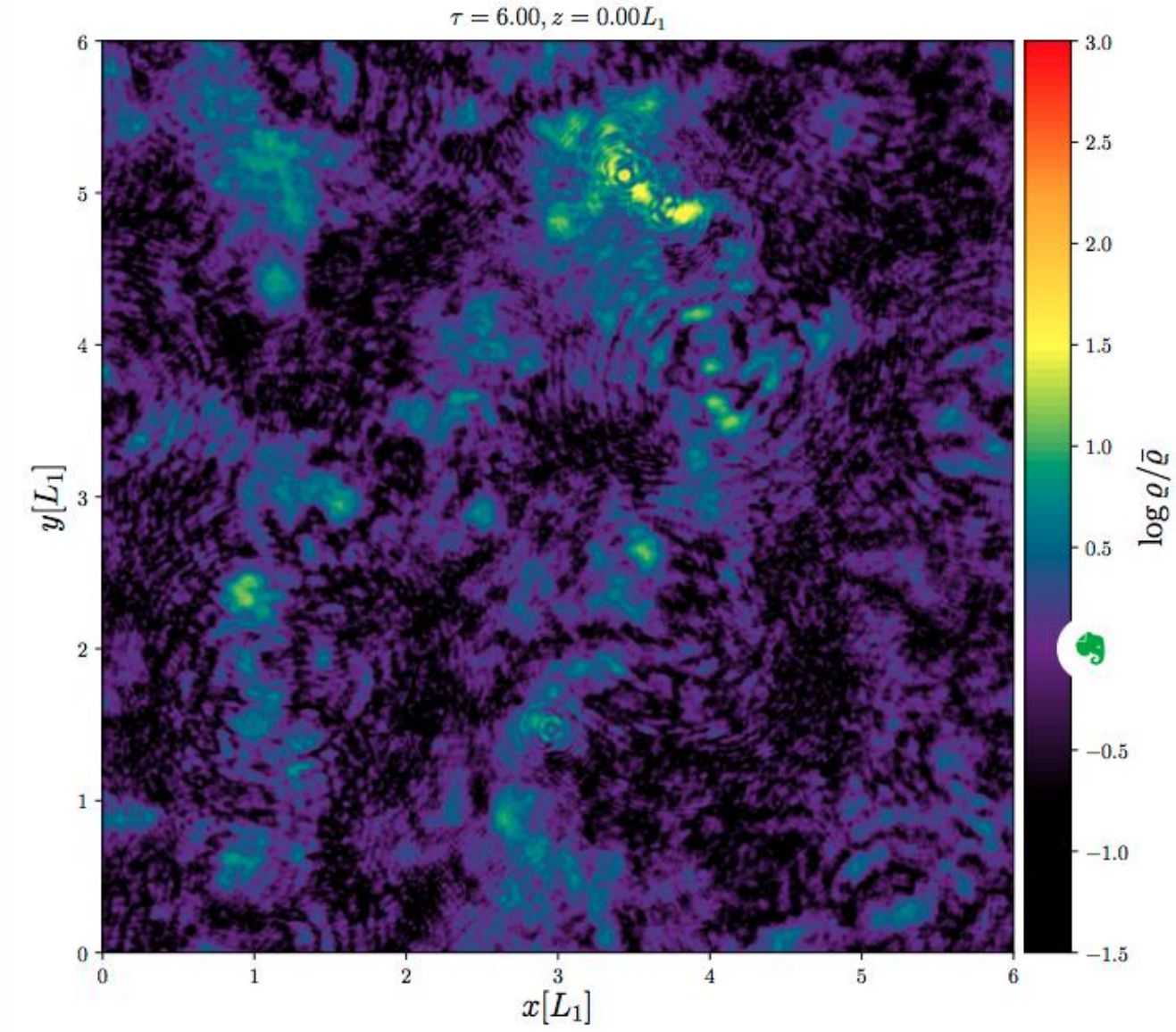

Vaquero et al (2018)

N-body sims: Wiebe, Brilenkov Master theses (U. Göttingen).

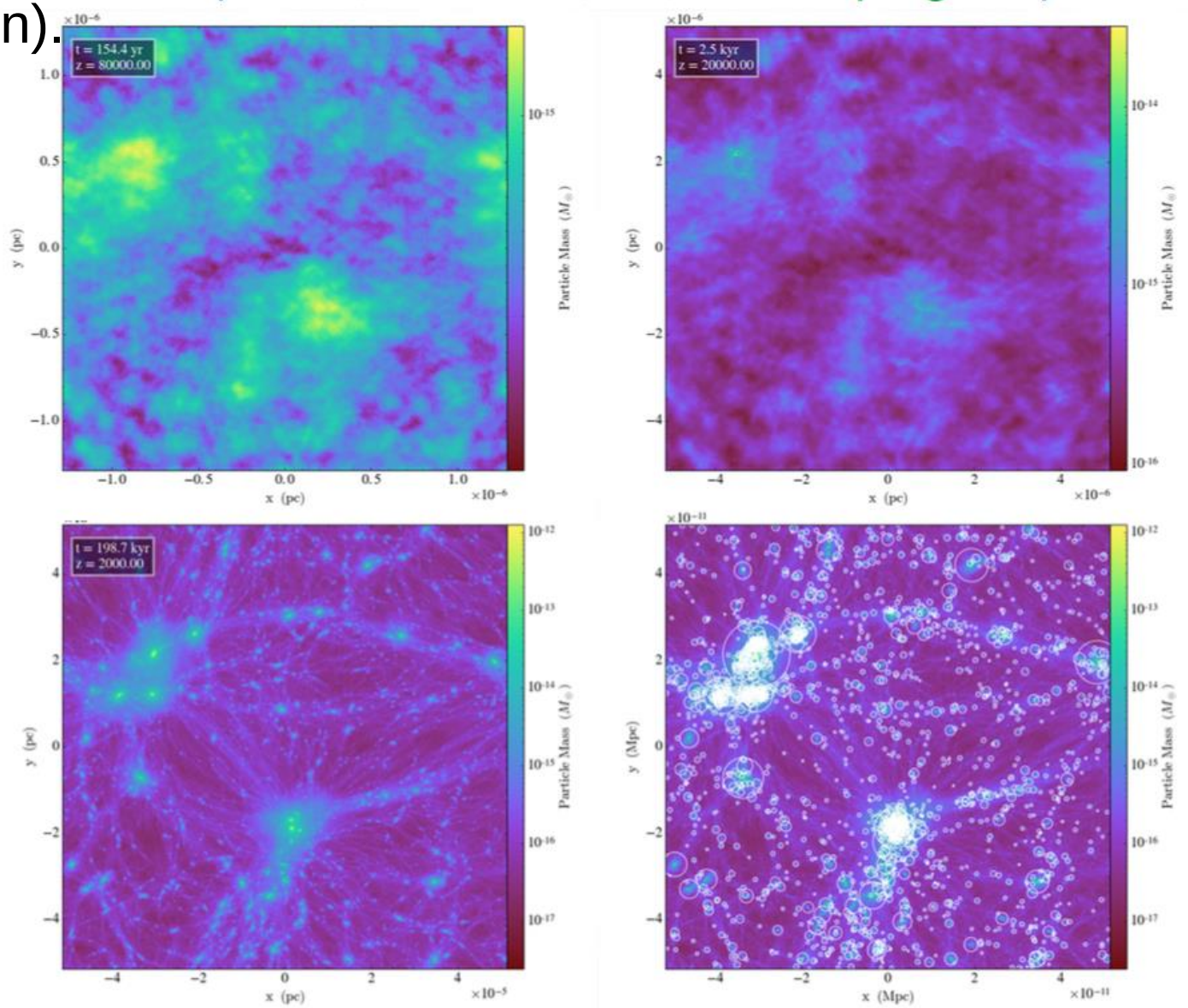

Observe power law mass fn near M_0, and power law $\rho(r) \sim r^{-2.5}$.

Collapse & Clustering

Large overdensities → small, tightly bound objects, assumed to survive into the present → “MACHO-like” inside galaxies.

1. Minicluster seed mass function?
2. Minicluster density profiles?
3. Mergers and “minicluster halos”?
4. Survival probability → final fMC?

1, 2, and 3 can be solved either using semi-analytic models, or simulation (N-body, or “FDM-like” to find axion stars).

4 can only be solved with semi-analytic models or idealised simulations (huge hierarchy between minicluster and MW mass).

Density and Radius

Spherical collapse in the radiation dominated era gives virial density:

$$\rho_{\rm vir} = 140(1+z_c)^3 \bar{\rho}_a \delta^3 (1+\delta)$$

Collapse occurs at a redshift zc, which can be earlier than equality.

Virial overdensity and collapse redshift set by initial overdensity.

“Large δ → earlier equality in the patch”.

Minicluster radius fixed by mass + virial overdensity:

$$M_{\rm MC} = \frac{4}{3}\pi \rho_{\rm vir} R_{\rm vir}^3$$

$$R_{\rm vir} \approx \frac{3.2\times 10^{-6}\ {\rm pc}}{\delta(1+\delta)^{1/3}} \left(\frac{M_{\rm MC}}{10^{-12} M_\odot}\right)^{1/3} \left(\frac{0.73\ {\rm eV}}{T_c}\right)^{4/3}$$

Axion field dynamics (simulation) → distribution of different values of δ → distribution of different initial sizes & masses.

Wide, non-Gaussian distribution of overdensities.
Well fit by “Pearson VII” distribution.

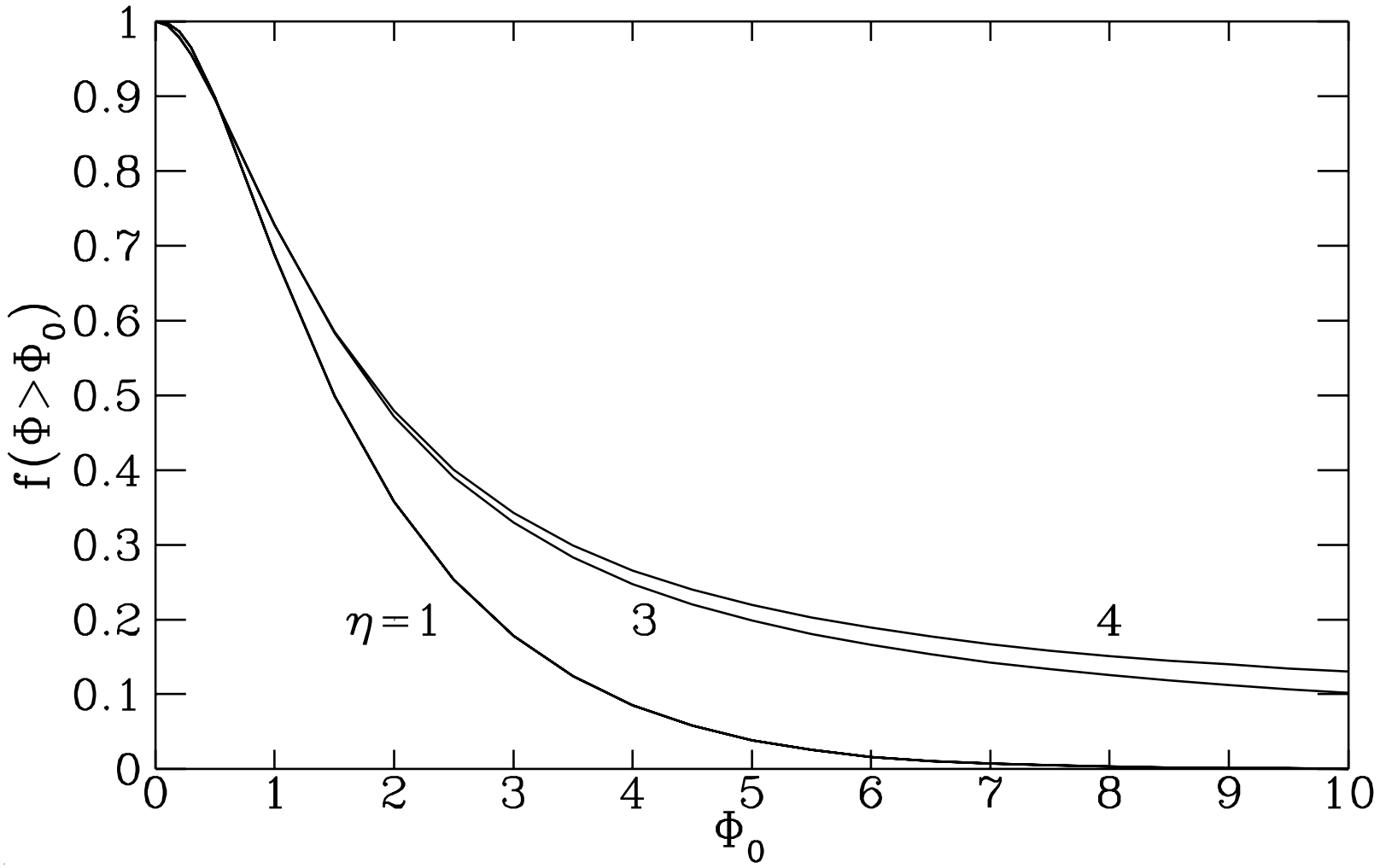

Kolb & Tkachev (1996)

Density and mass are correlated in initial conditions by thresholding. Need gravitational simulations to observe virialisation.

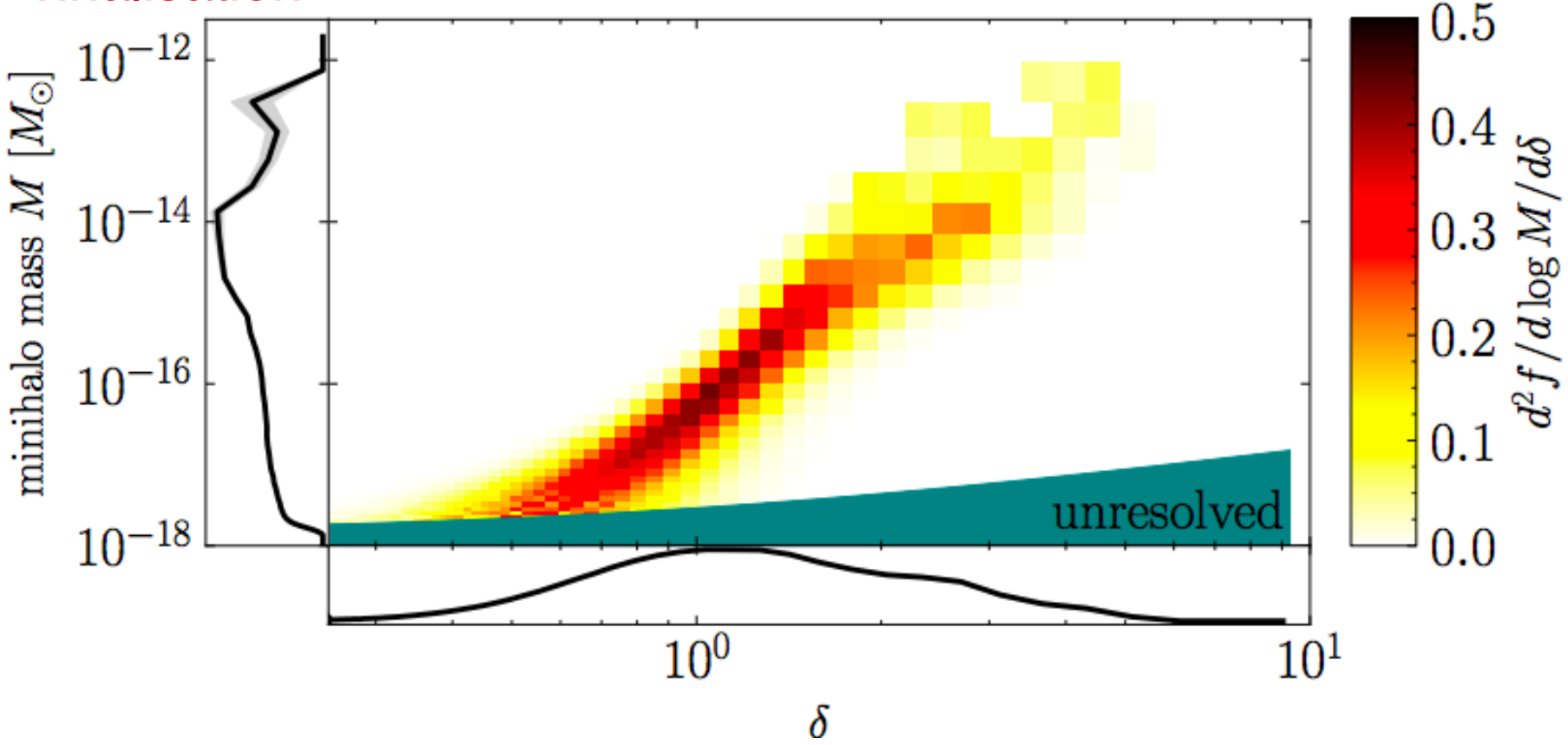

Buschmann, Foster & Safdi (2019)

Density Profile

Self-similar infall of top-hat profiles → $\rho \sim r^{-9/4}$ profile.
Realistic collapse in an environment → NFW-like profiles.
Q: how do we use δ to define the minicluster radius?

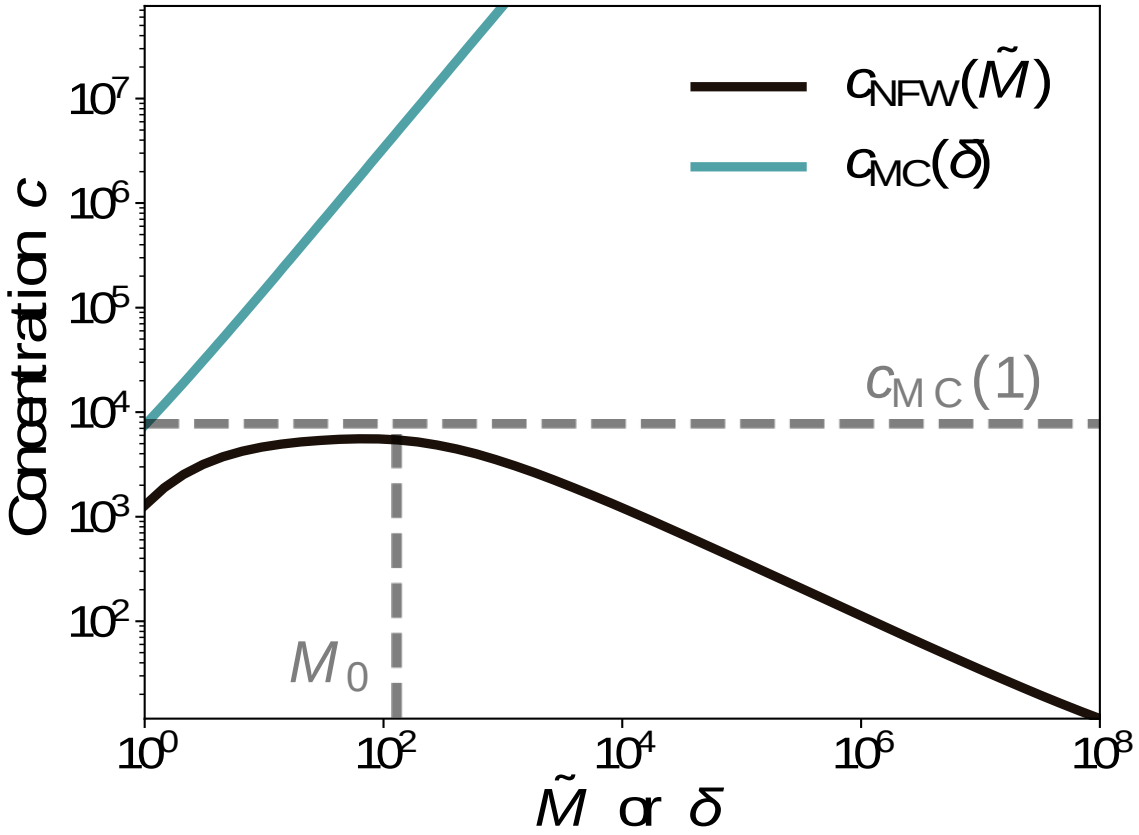

Hierarchical Press-Schechter model from δ~1 seeds → diffuse "minicluster halos".

Seeds only, Kolb & Tkachev δ distribution

Axion Stars in Miniclusters

Just like FDM, cooling + gradient pressure → soliton formation.

FDM-like core-halo mass relation observed to be obeyed.

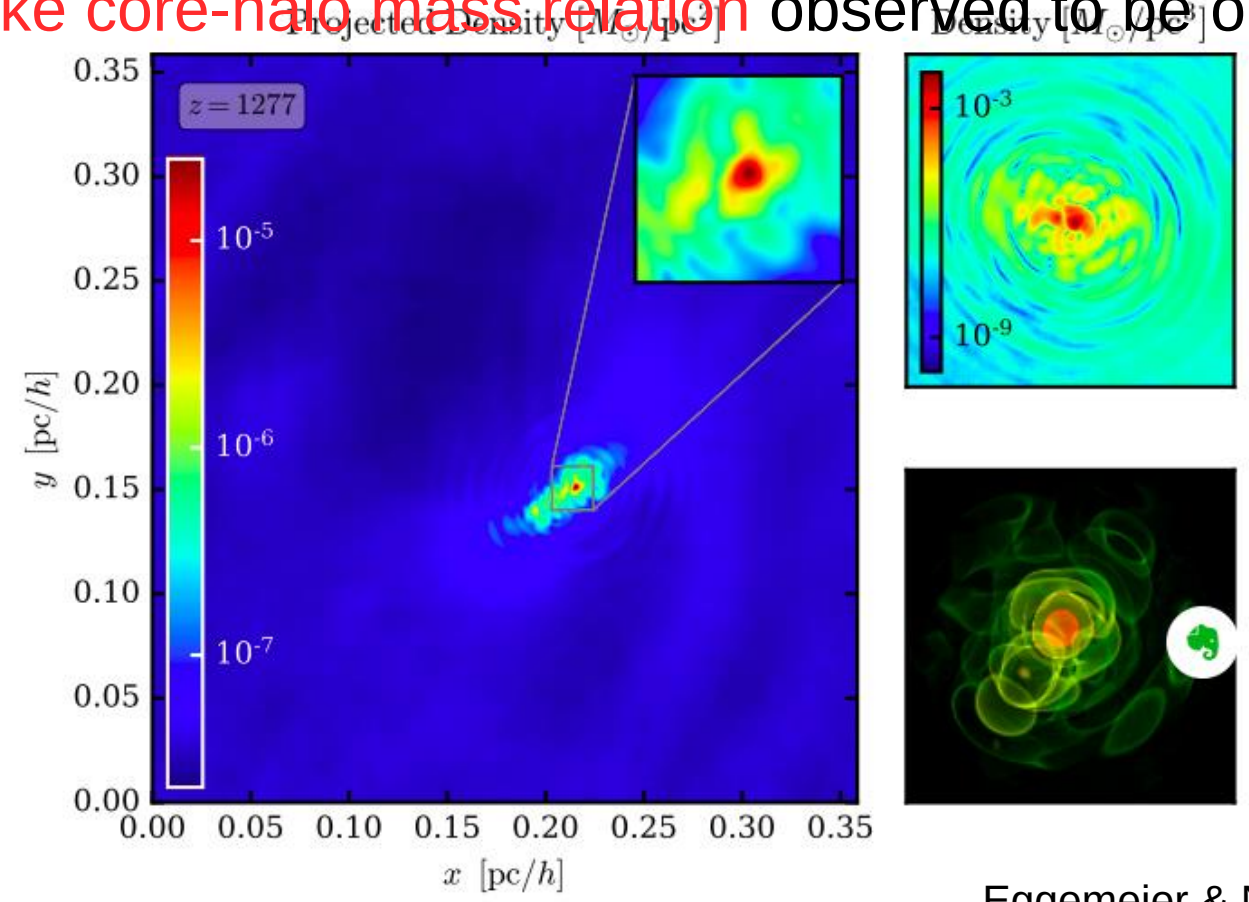

Eggemeier & Niemeyer (2019)

Tidal Stripping?

Dokuchaev et al (2017)

1. Model infall of miniclusters into host galaxy.
2. Survival probability increases for steeper profiles and larger δ.
3. Processes initial fMC → fMC(l,b) galactic co-ordinates.
4. Are de… …er layers

Not studied!

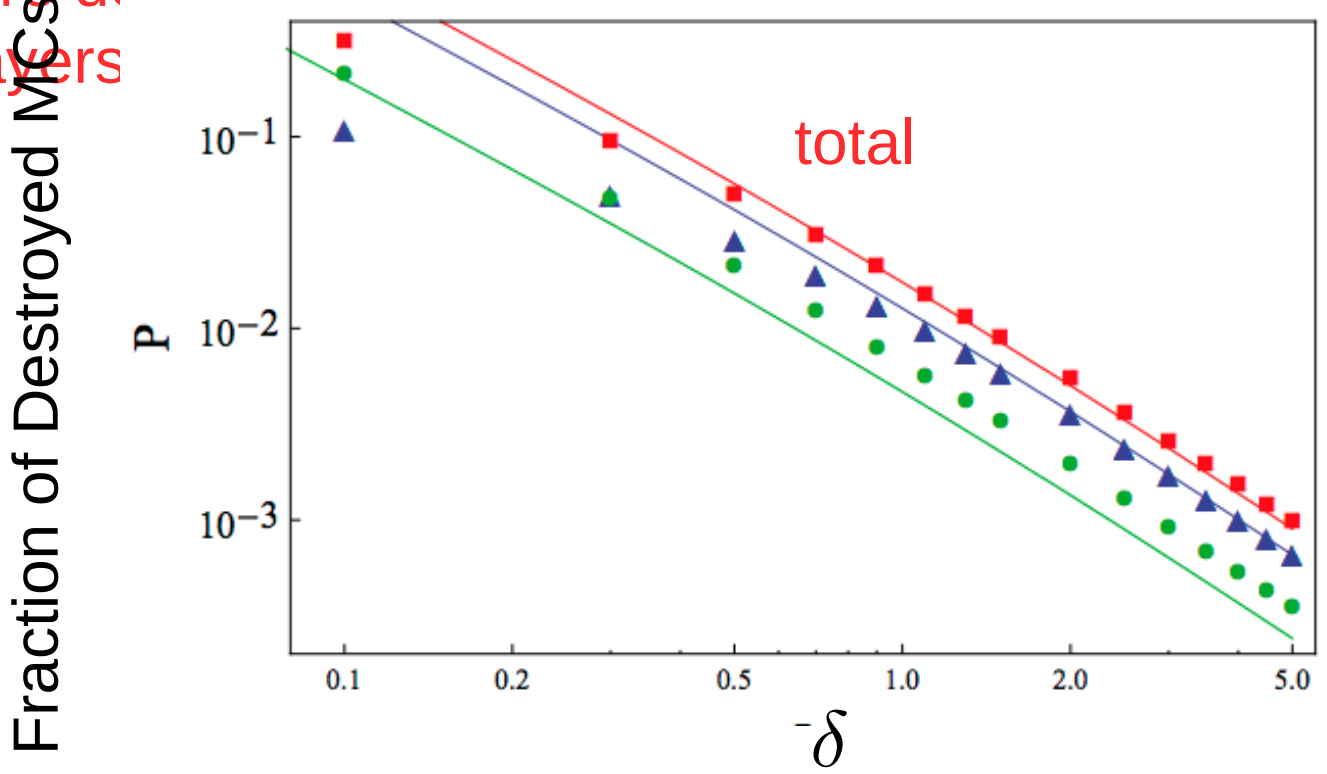

Gravitational Microlensing

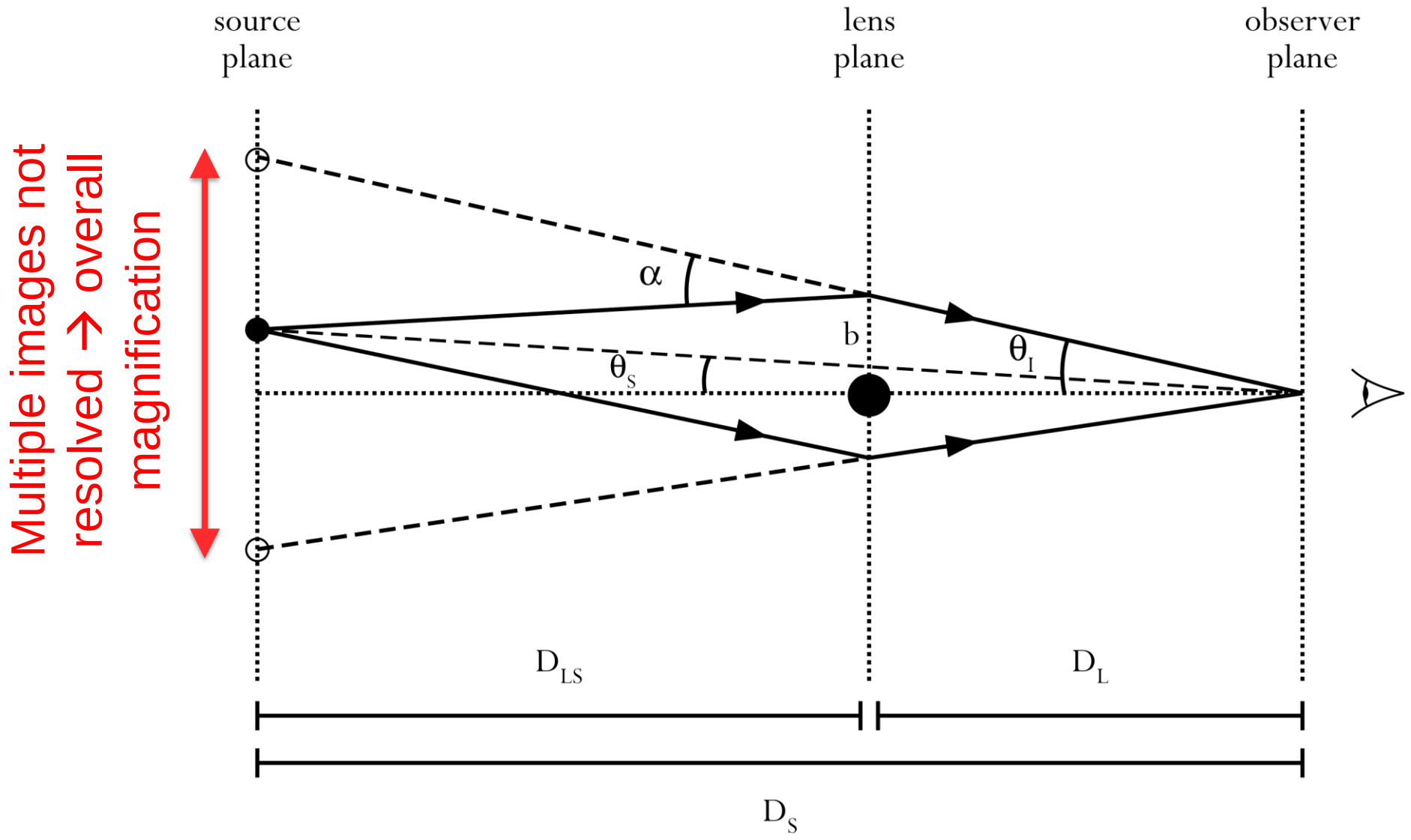

Gravitational Microlensing

Griest (1991)

$$A(u) = \frac{u^2 + 2}{u(u^2 + 4)^{1/2}} \qquad R_{\rm E}(x, M) = 2[GMx(1-x)d_s]^{1/2}$$

Define the “microlensing tube” where A>1.34 → “event”:

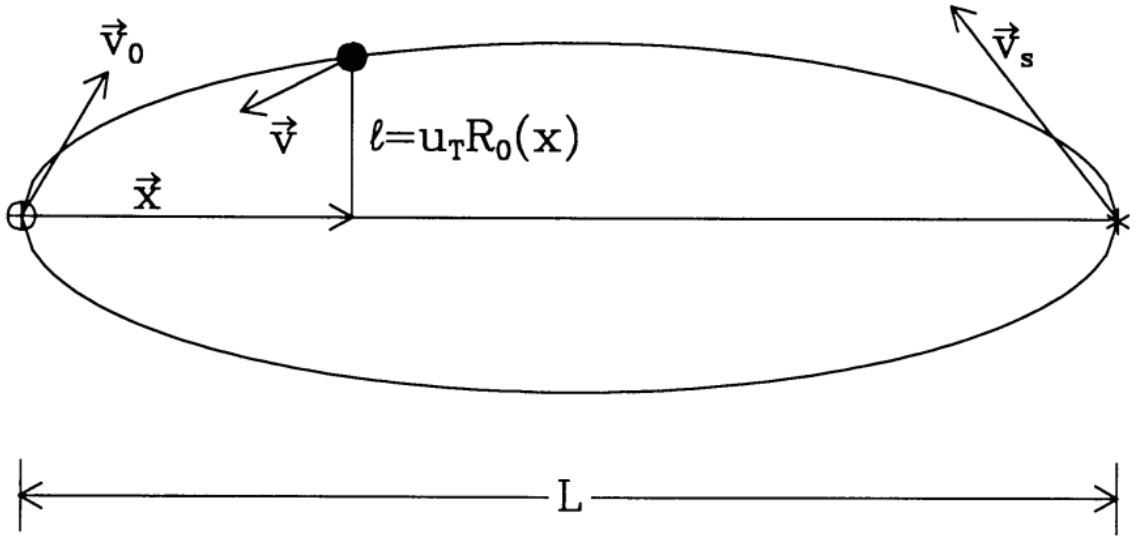

FIG. 1.—Microlensing “tube,” variables, and velocities. The observer is marked ⊕, the source by an asterisk, and the dark matter object by a filled circle. A dark matter object inside the tube constitutes an “event”.

For a given host halo model, one can compute the event rate from lenses crossing this tube.

Constraints on PBHs

Niikura et al (2018)

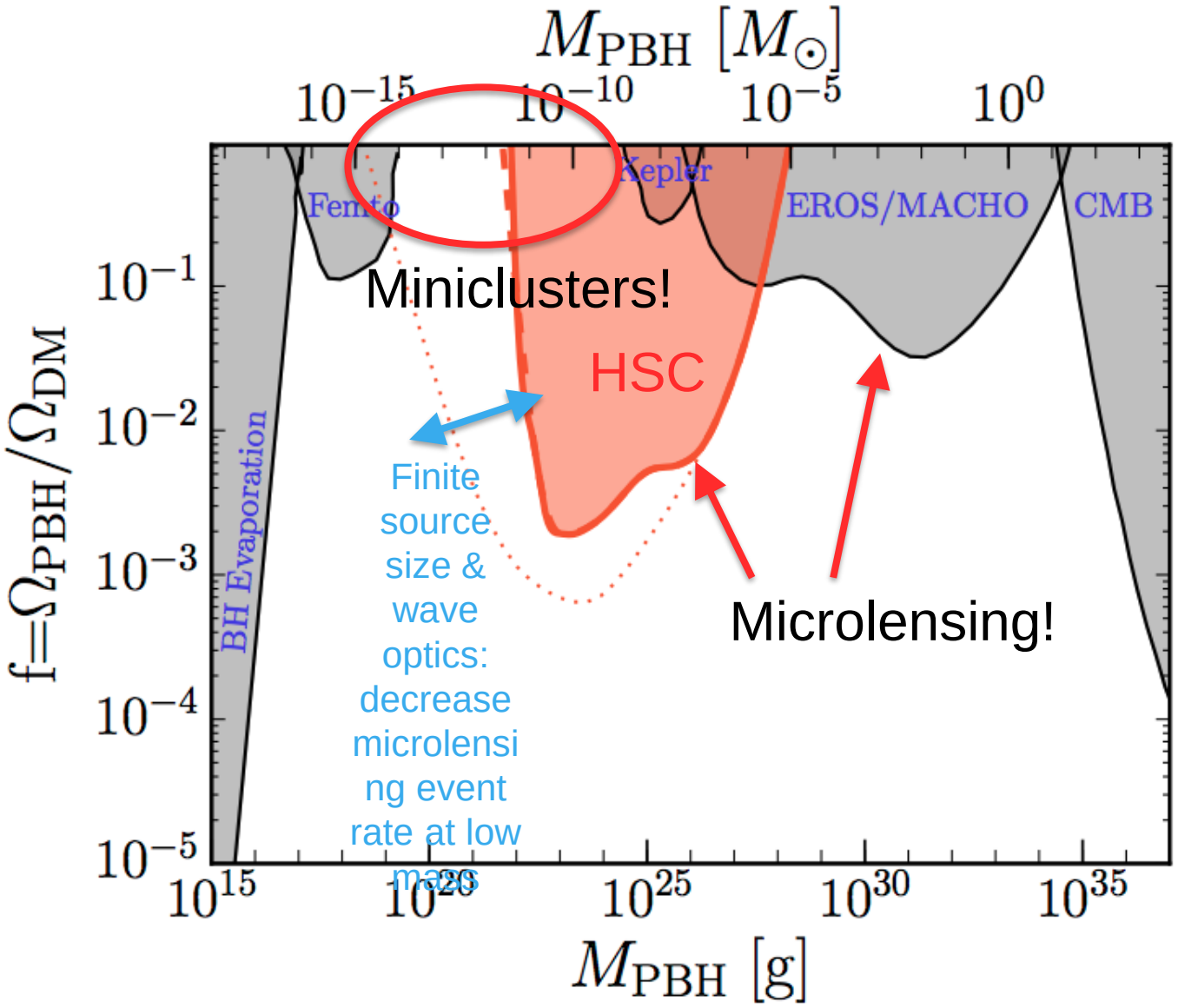

Lensing with Density Profiles

Non-point sources do not lens as much as PBHs.
Model miniclusters density profile and use eqns:

$$A = [(1 - B)(1 + B - C)]^{-1}$$

$$C = \frac{1}{\Sigma_c \pi \ell} \frac{\mathrm{d}M(\ell)}{\mathrm{d}\ell} \; ; \; B = \frac{M(\ell)}{\Sigma_c \pi \ell^2} \; ; \; \Sigma_c = \frac{1}{4\pi G d_s x(1-x)}$$

Approximate:
lensing tube is rescaled:

$$R_{\mathrm{MC}}(x, M, \delta) = \mathcal{R}(\delta, M) R_E(x, M)$$

Behave like point mass when scale radius ~ R_E
→ need large M or δ

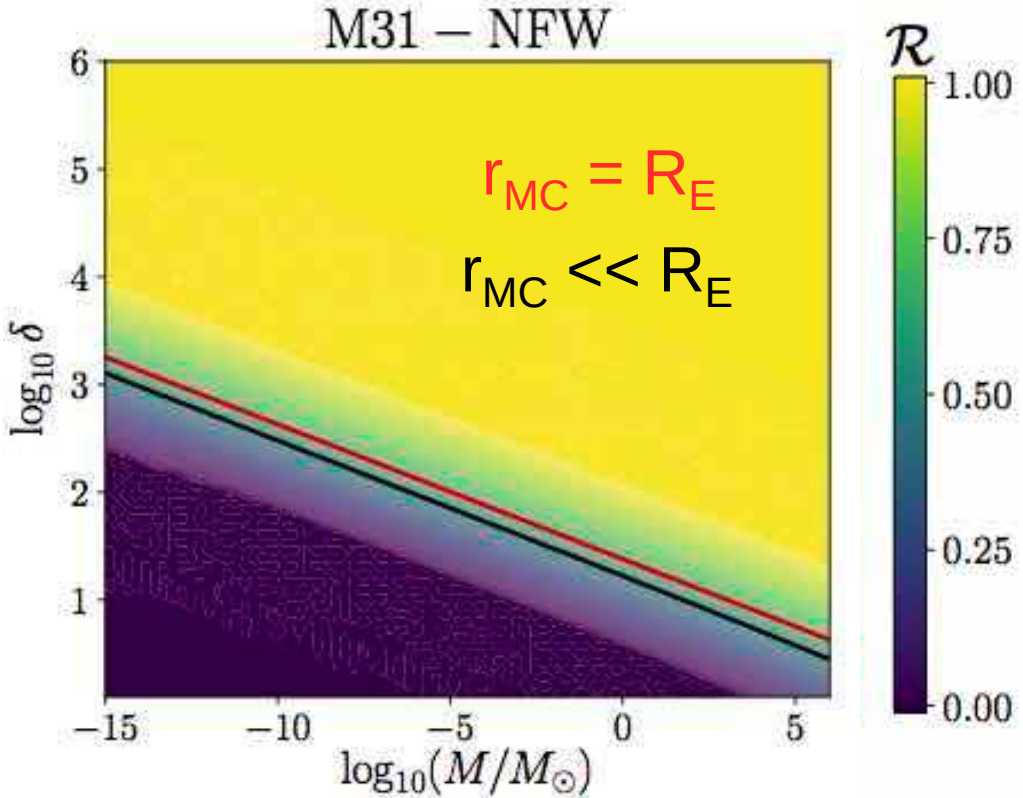

Lensing Events

Rate for lenses to cross the tube in dt towards a given source, d_s.

For a distribution of lenses, we integrate over the mass function:

$$\frac{\mathrm{d}\Gamma}{\mathrm{d}\hat{t}} = \frac{32 d_s}{\hat{t}^4 v_c^2} \int_0^\infty \left[\frac{\mathrm{d}n}{\mathrm{d}\ln M} M \int_0^\infty \rho_{\mathrm{host}}(x) R_{\mathrm{E}}^4 e^{-4R_{\mathrm{E}}^2/(\hat{t}^2 v_c^2)} \right] \mathrm{d}M$$

Similarly for a distribution of density profiles.

Integrate the event rate with $R_E \rightarrow R_{MC}$ over $dn/d\delta$ (from fit):

$$\frac{\mathrm{d}\Gamma}{\mathrm{d}\hat{t}} = \int_0^\infty \mathrm{d}\delta \frac{\mathrm{d}n}{\mathrm{d}\delta} [\cdots]_{\mathrm{MC}}$$

$$N_{\mathrm{exp}} = E \int \mathrm{d}\hat{t} \epsilon(\hat{t}) \frac{\mathrm{d}\Gamma}{\mathrm{d}\hat{t}}$$

Exposure, E

efficiency, ε

Assuming NFW profile and Dirac-δ mass distribution, but ignoring finite source size and wave optics: significant if $M_{MC}<10^{-11}M_{\odot}$

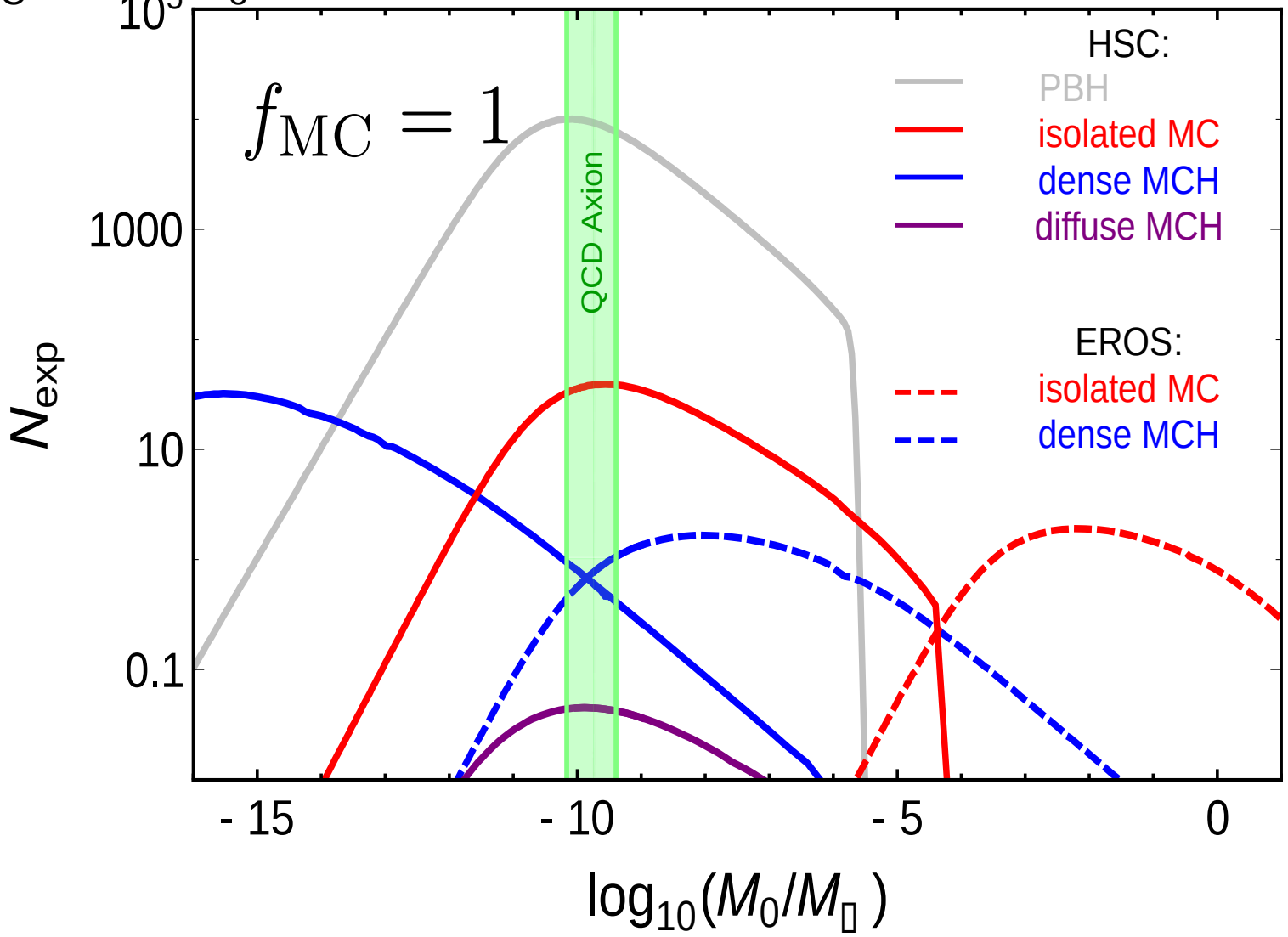

No observed events → Poisson stats 95% C.L. exclusion on fMC

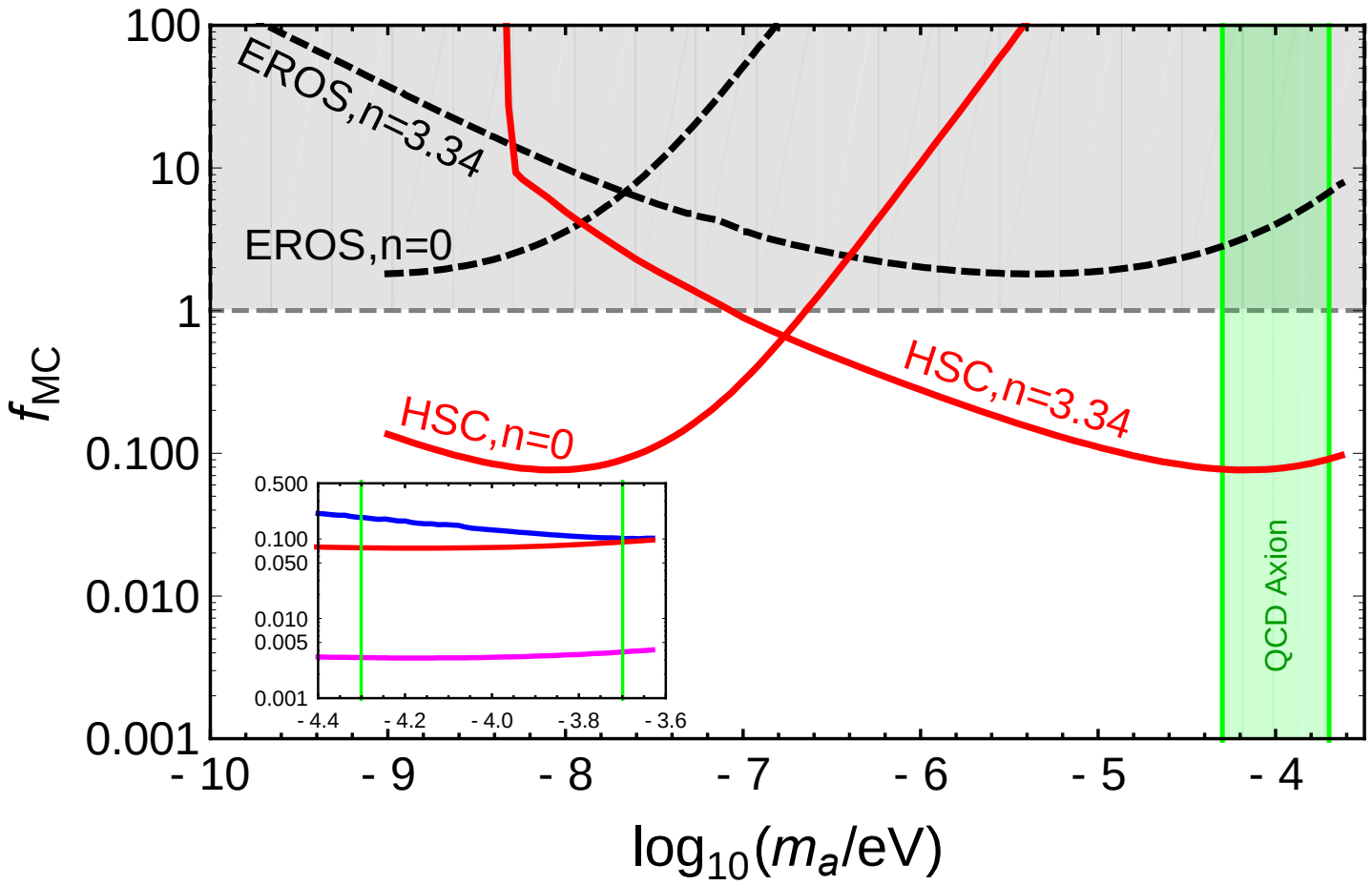

Better predictions for M0, ρ(r), and fMC needed.

1. Have we already constrained the QCD axion in classic window?
2. How will observations improve in the future?

Miniclusters in Haloscopes

Tidal streams observable in haloscope spectrum

O'Hare & Green (2017)

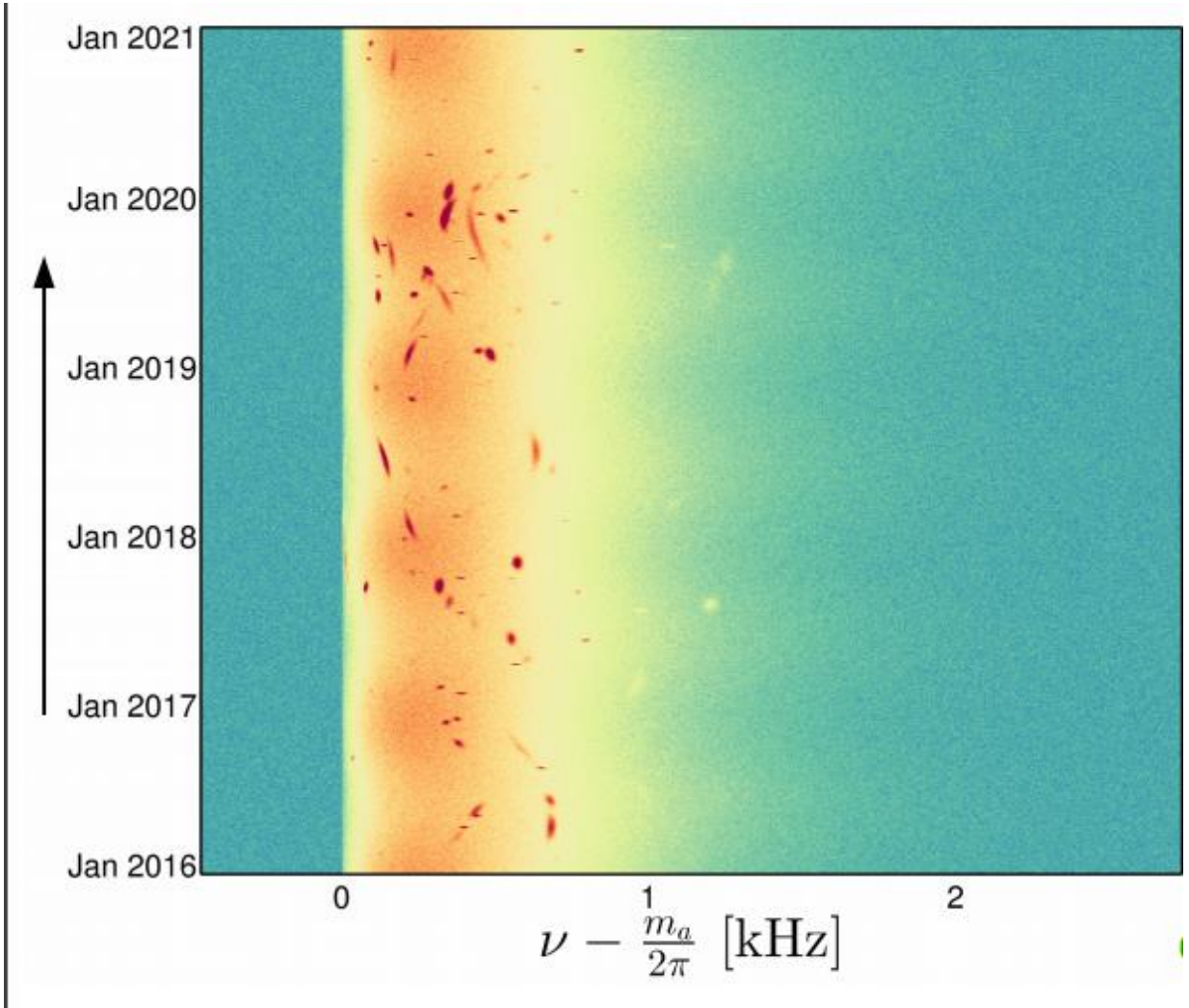

DETECTING HEAVY AXIONS

See Ringwald’s talk

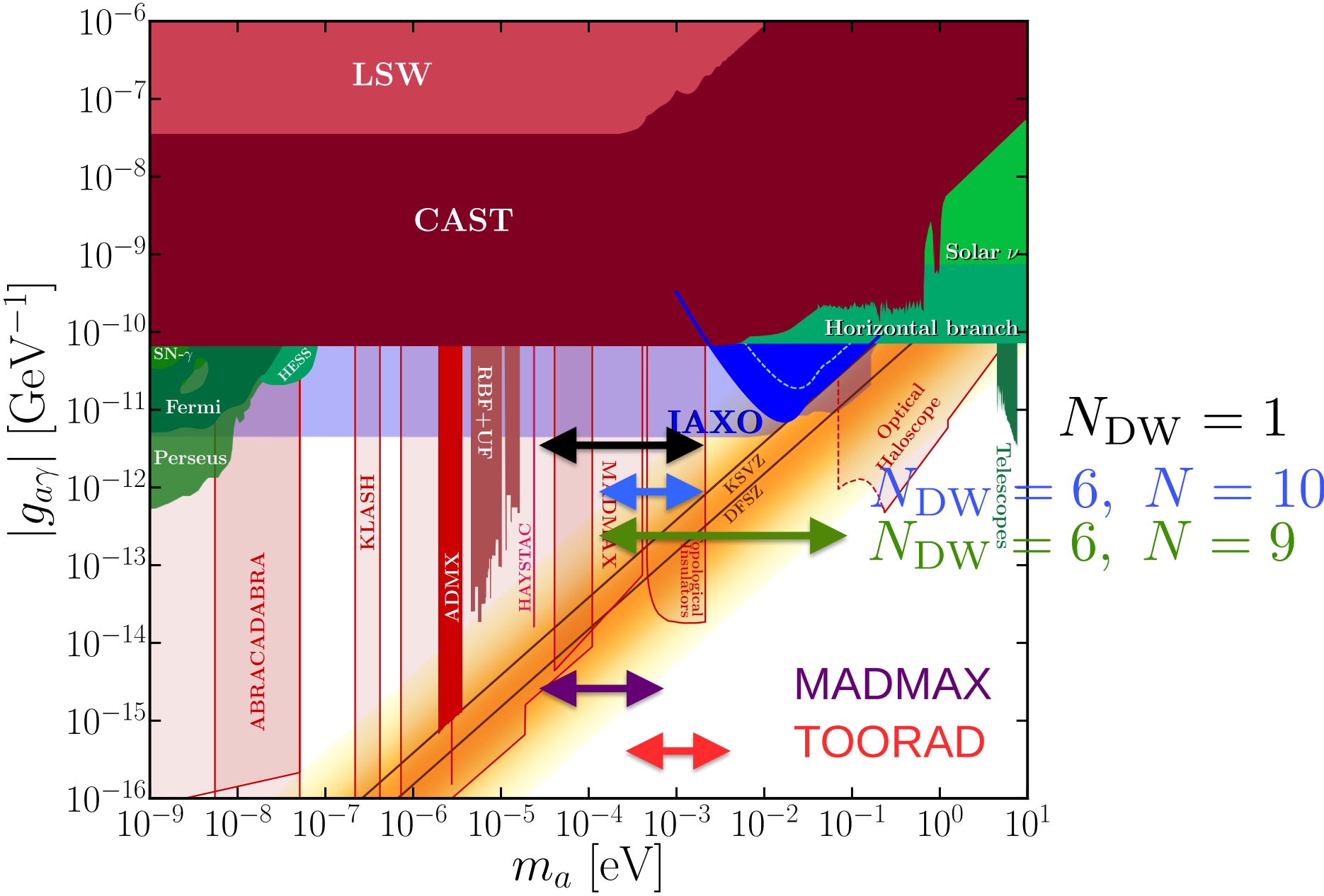

Fig: Dafni et al (2019)

Radio Astronomy

Hook et al (2018); Dietrich et al (2018); Huang et al (2018); Edwards et al (2019)

Axion conversion occurs in NS magnetosphere → radio line.

Minicluster collision → transient.

Axion star io.

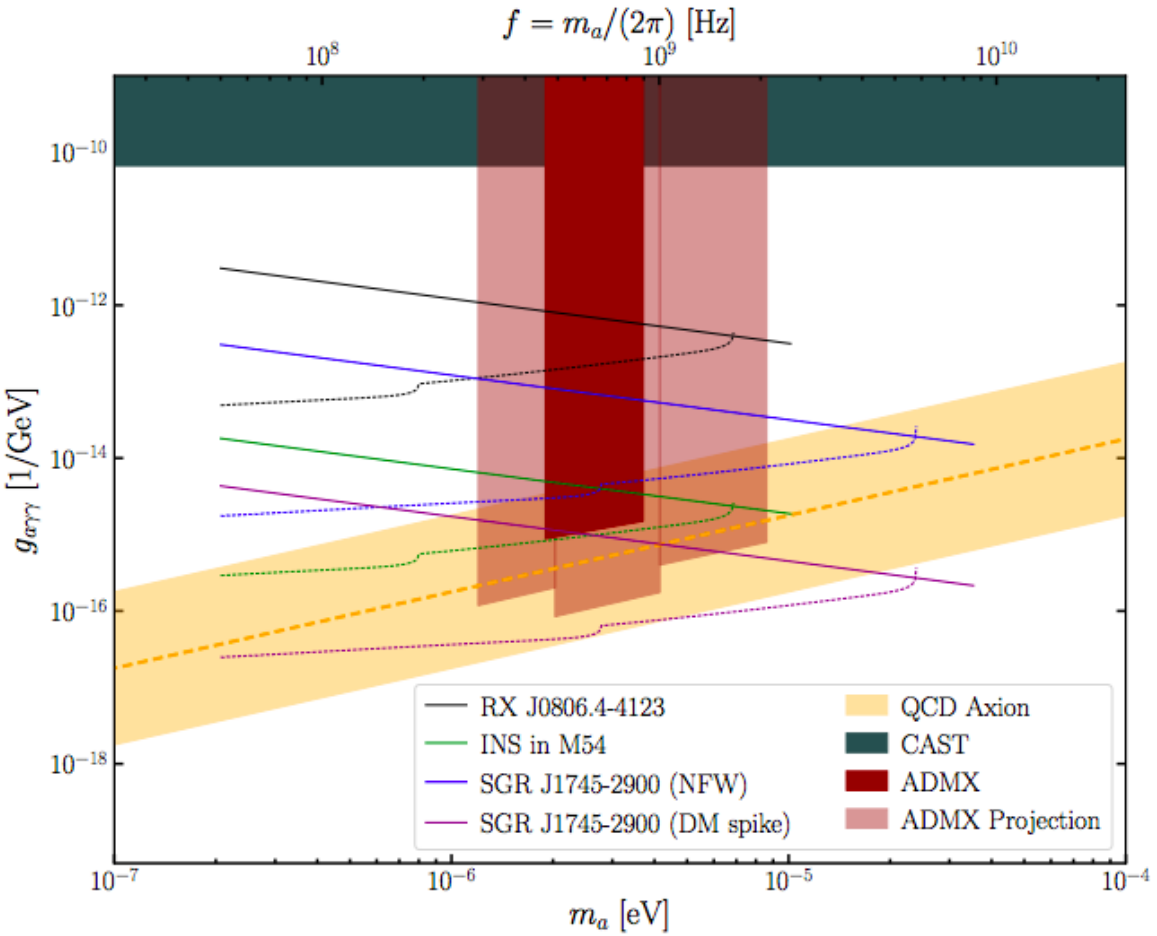

Radio Astronomy & Haloscopes

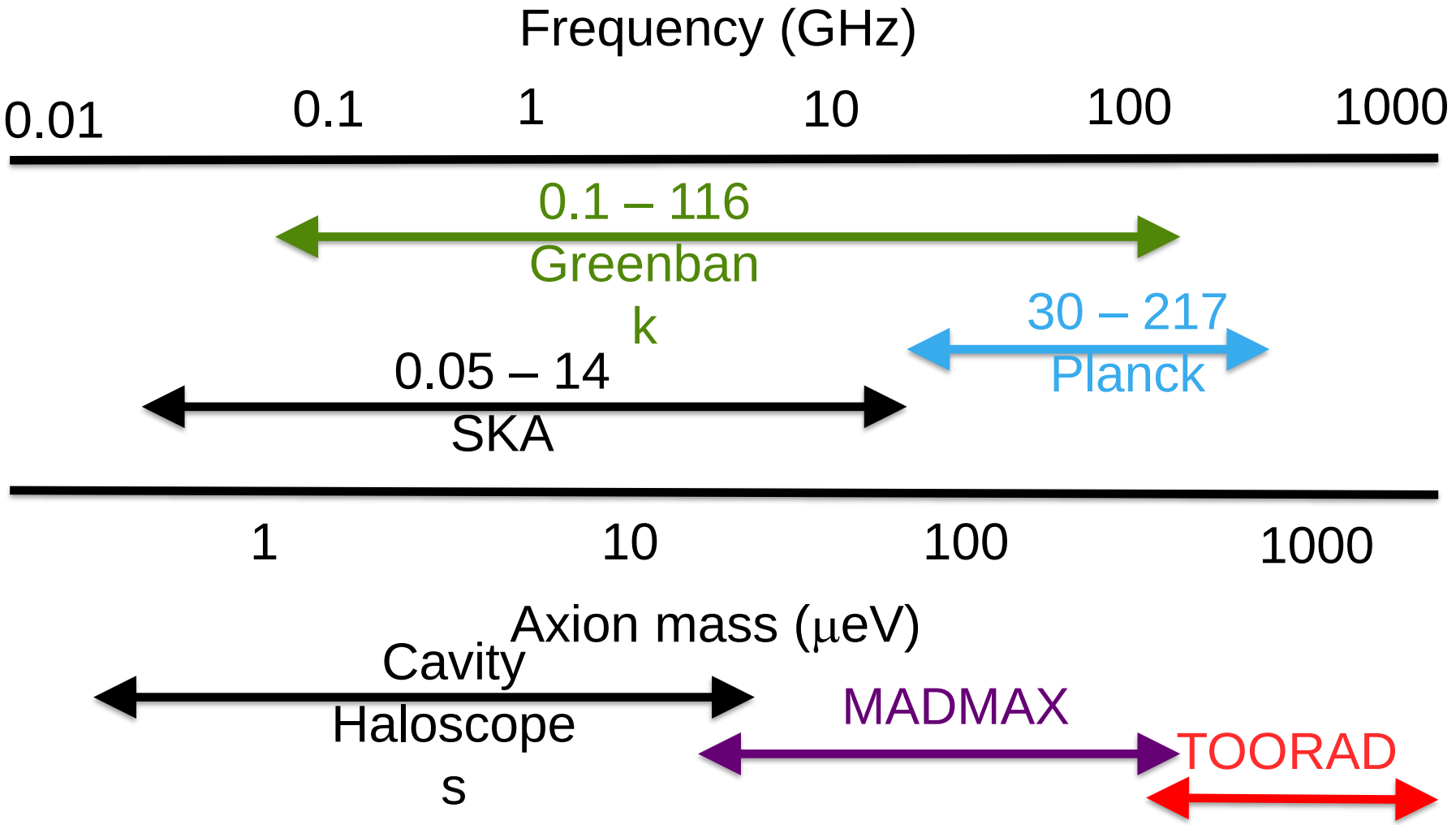

MADMAX: Dielectric Haloscope

Coherent induced EM from dielectric boundary → enhancement.
Prototype built in Munich. Full experiment funded at DESY.

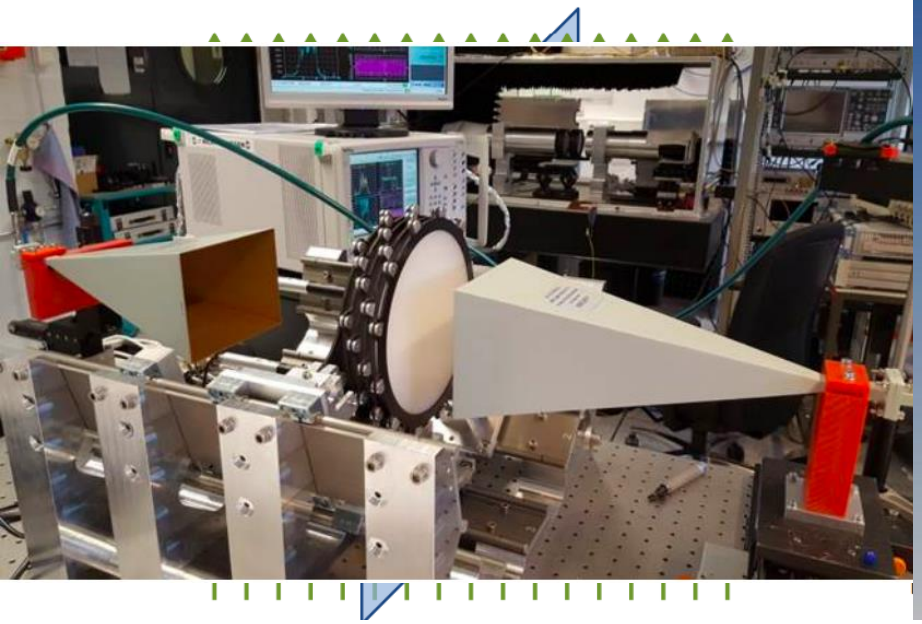

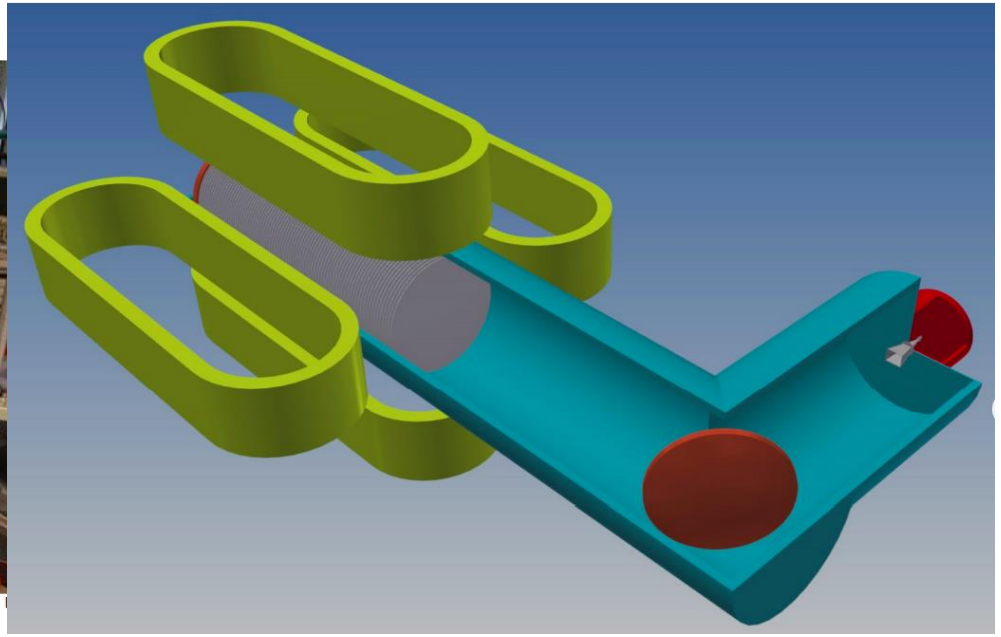

MADMAX interest group (2017)
Horns et al (2013)

The MADMAX Magnet

BILFINGER

- Weight: < 200.000 Kg
- Length: 6900 mm
- Diameter: 4400 mm
- Warm bore: 1350* mm
- Superconducting cable: 35.000 m
- Superconducting wire: > 700.000 m NbTi
- Operating temperature: ~2 K

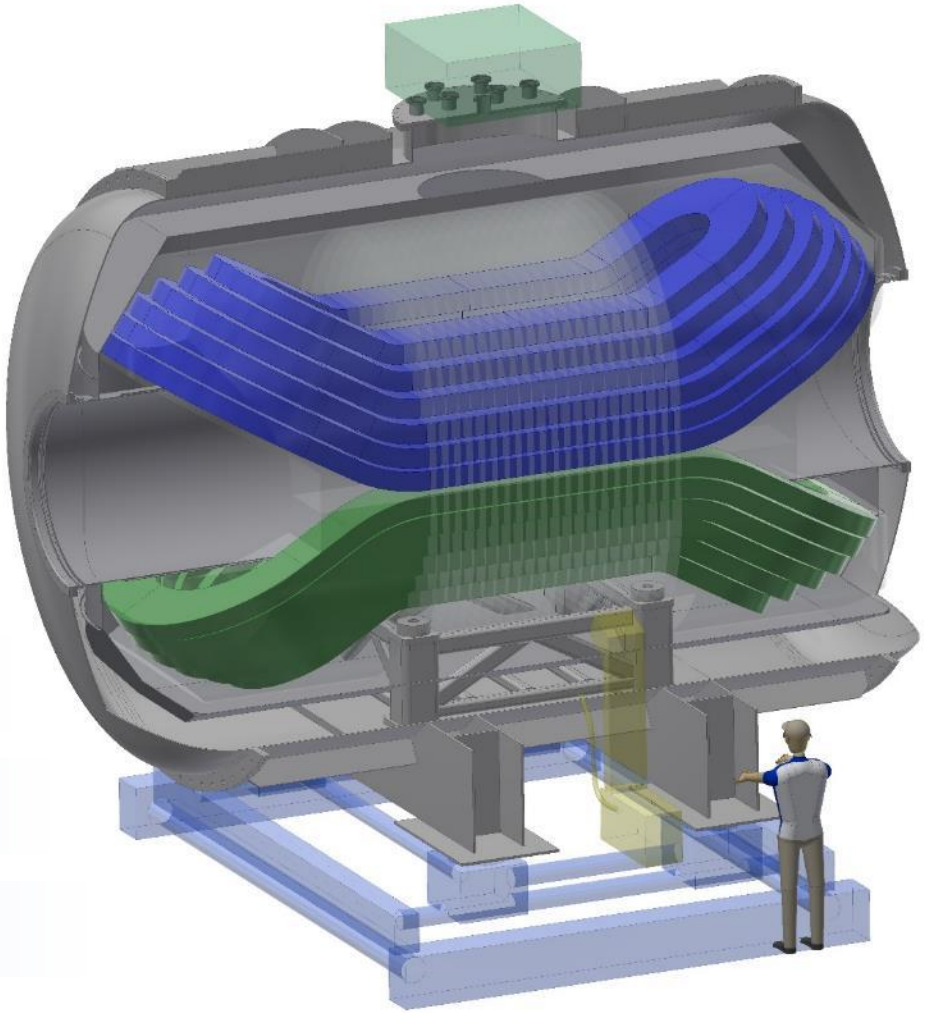

To be housed in HERA yoke at DESY.

MADMAX: Dielectric Haloscope

Projected sensitivity to heavier axions than RF cavities:

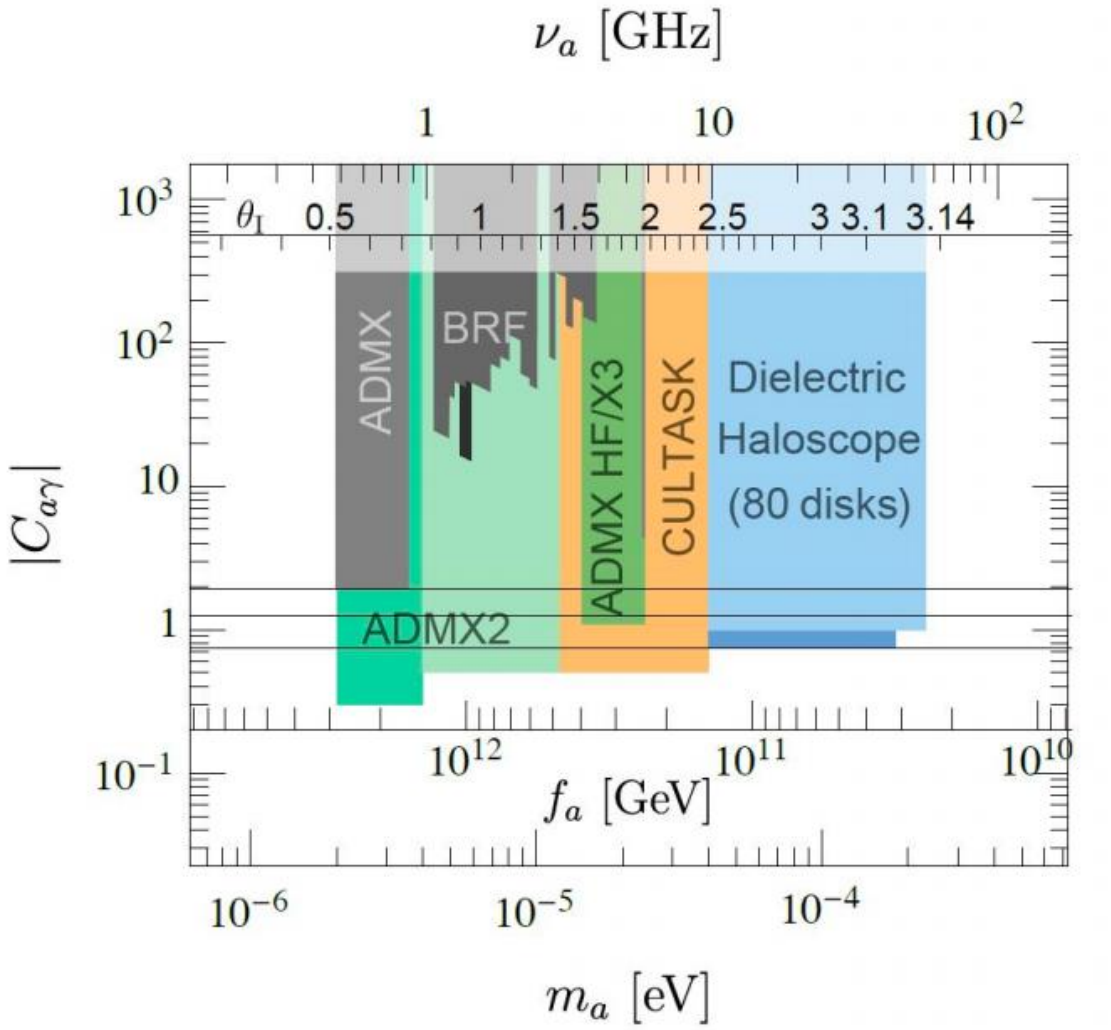

Millar et al (2016)

“TOORAD”: TOpOlogical Resonant Axion Detection
arXiv:1807.08810 (still under review, PRL)

GEORG-AUGUST-UNIVERSITÄT GÖTTINGEN

Unterstützt von / Supported by

Alexander von Humboldt Stiftung/Foundation

Mazhar Ali

Erik Lentz

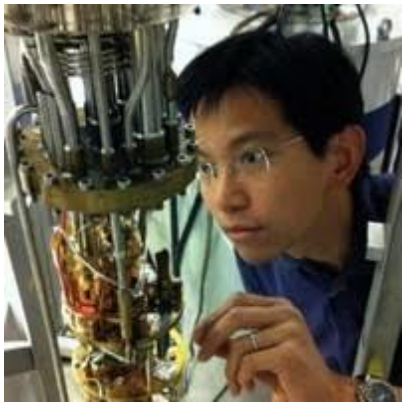

Kin-Chung Fong

Libor Smejkal

Chris Weber

MAX-PLANCK-GESELLSCHAFT

BBN TECHNOLOGIES

JG|U

NSF

ARTICLES
PUBLISHED ONLINE: 7 MARCH 2010 | DOI: 10.1038/NPHYS1534
nature physics

Dynamical axion field in topological magnetic insulators

Rundong Li[1], Jing Wang[1,2], Xiao-Liang Qi[1] and Shou-Cheng Zhang[1]*

Axions are weakly interacting particles of low mass, and were postulated more than 30 years ago in the framework of the Standard Model of particle physics. Their existence could explain the missing dark matter of the Universe. However, despite intensive searches, axions have yet to be observed. Here we show that magnetic fluctuations of topological insulators couple to the electromagnetic fields exactly like the axions, and propose several experiments to detect this dynamical axion field. In particular, we show that the axion coupling enables a nonlinear modulation of the electromagnetic field, leading to attenuated total reflection. We propose a new optical-modulator device based on this principle.

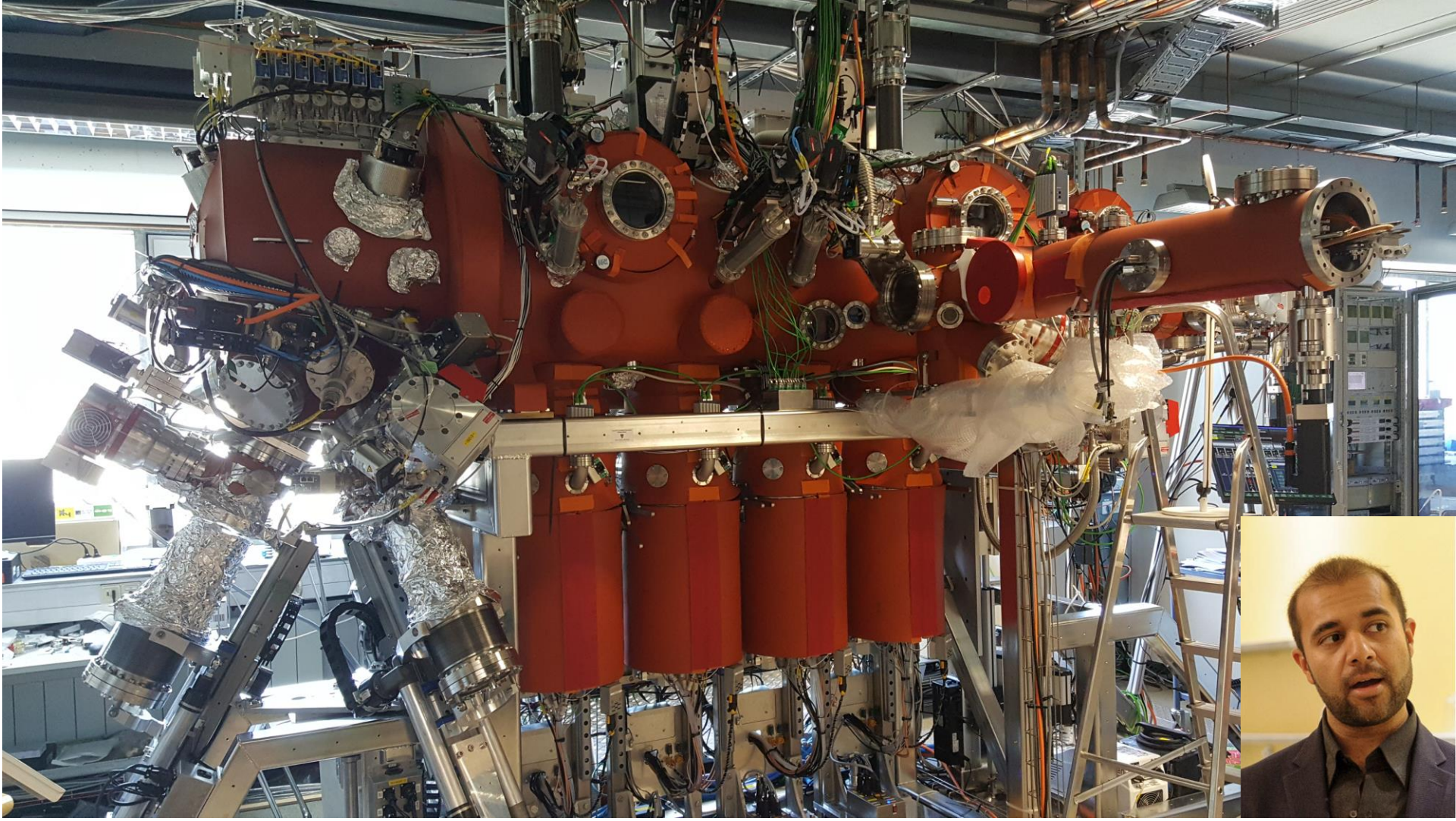

Making thin film heterostructures.

“Mango”: hybrid deposition tool. MPI Microstructure Physics, Halle.

Condensed matter: Chern-Simons term is in magneto-electric materials.

If T (and thus CP) is conserved, the θ term is locked to 0 or π.

This effect is predicted to occur in topological insulators, with

Qi, et al (2008)

$$\theta = \frac{1}{4\pi}\int \mathrm{d}^3k\epsilon^{ijk}\mathrm{Tr}\left[A_i\partial_j A_k + i\frac{2}{3}A_iA_jA_k\right] \qquad A_i^{\alpha\beta}(\vec{k}) = -i\langle\alpha\vec{k}|\partial/\partial k_i|\beta\vec{k}\rangle$$

Chern-Simons form

Berry phase gauge field for Bloch wavefunctions in band α.

Electronic structure (TI bands) → Chern-Simons term

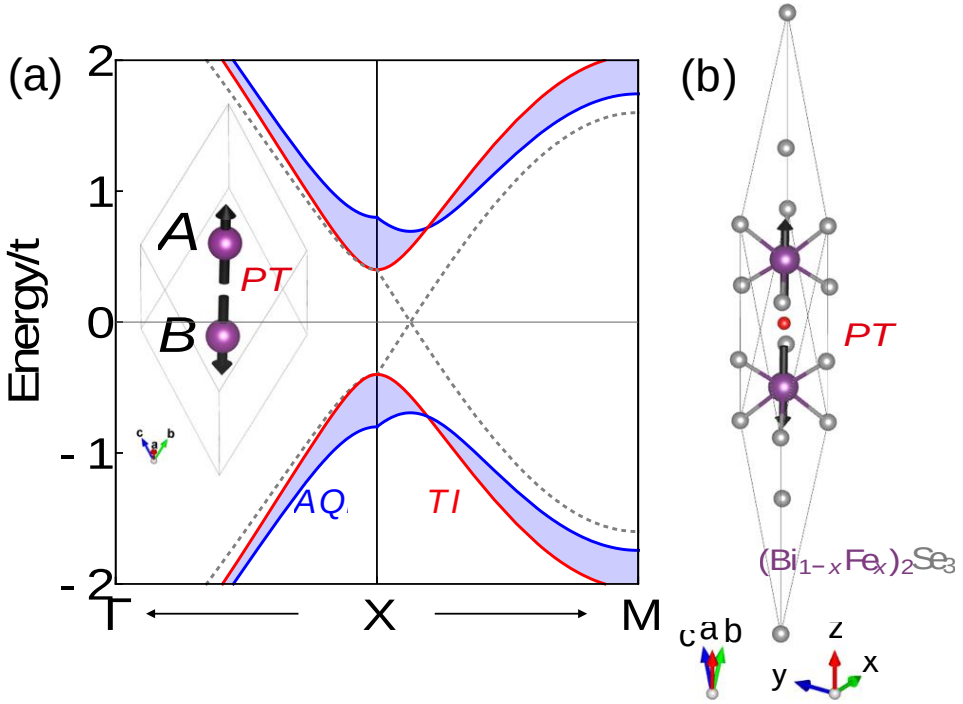

If time-reversal symmetry can be broken → dynamical “anaolgue axion”.

Local fluctuations in θ caused by spin-induced shifts in band energies:

$$\mathcal{L}_{\mathrm{AQ}} = \frac{f_Q^2}{2}\left[\dot{\theta}_Q^2 - (v_{s,i}\partial_i\theta_Q)^2 - m_Q^2\theta_Q^2\right] + \frac{\alpha}{2\pi}\theta_Q E\cdot B$$

Spin desnity waves e.g. in Fe doped Bi_2Se_3. Li et al (2010)

$$\delta\theta_Q \sim \frac{2}{3}\sum U m_i$$

Spin-wave Néel vector fluctuation.
Z = bulk magnetization direction

Electronic structure (TI bands) → Chern-Simons term → compute AQ “decay constant”

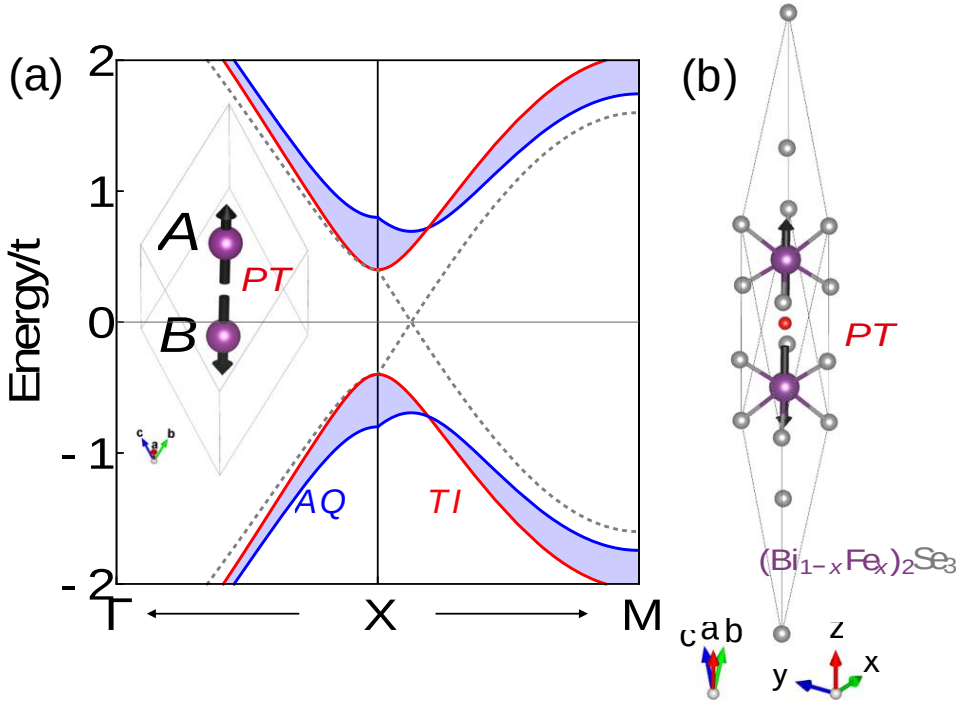

AF fluctuations between sub-lattice A,B → pseudoscalar spin waves coupled to CS

Low energy EOMs for E-field and AF-magnon θ_Q (no electrons):

$$\epsilon\ddot{\mathbf{E}} - \nabla^2\mathbf{E} + \frac{\alpha}{\pi}[\mathbf{B}_0\ddot{\theta}_Q - \nabla(\nabla\theta_Q \cdot \mathbf{B}_0)] = \mathbf{A}\cos\omega_a t$$

$$\ddot{\theta}_Q - v_Q^2\nabla^2\theta_Q + m_Q^2\theta_Q - \frac{\alpha}{4\pi^2 f_Q^2}\mathbf{B}_0 \cdot \mathbf{E} = 0$$

Our observation: dark matter axions source an E-field inside the material.

The presence of the Chern-Simons term couples E-field to spin waves via mass mixing (linear).

The spin wave has a mass set by anti-ferromagnetic exchange. Larmour frequency ~ 1 meV.

Axion-Polaritons

Diagonalise the equations of motion to find ϕ propgating d.o.f.

$$\omega_{\pm}^2(k) = (k^2/\epsilon^2 + m_Q^2 + b^2) \pm \sqrt{(k^2/\epsilon^2 + m_Q^2 + b^2)^2 - 4k^2 m_Q^2/\epsilon^2}$$

Mixing parameters:

$$b^2 = \alpha^2 B_0^2/4\pi^3 \epsilon f_Q^2$$ photon mass term

$$f_+ = b^2/(\omega^2 + b^2)$$ fractional power in + mode

Good mixing requires $b \sim m_Q \sim \omega_a$ → need small $f_Q \sim 500$ eV.

Candidate Materials

Magnetically doped TI's: Li et al (2010); Sekine & Nomura (2014)

Dirac based. Fu-Kane model of AF-diamond (our model). e.g. Be_2Se_3, or $EuIn_2As_2$. Parameters known, not realised in the lab.

Intrinsic magnetic TIs: Zhang et al (2019)

New candidates, e.g. $Mn_2Bi_2Te_5$. Problem of doping SOC?

Charge density waves in Weyl materials: Gooth et al (2019)

e.g. $(TaSe_4)_2I$. Different mechanism → params could be v. different. Some practical evidence in the lab. Params unknown.

Magnetoelectrics with corundrum structure: Wang et al (2011);Wang et al (2019)

e.g. α-Cr_2O_3 (Chromia). Demonstrated axion term via optical measurements. Not symmetry protected → weak Chern-Simons term: f_Q~6400 eV → poor mixing.

Magnetic TI superlattices: Wang et al (2016);

Ni, Cr, Mn doped TI layers. Params seem poor (large f_Q).

AF Doped Bismuth Selenide

In our model we can directly compute $m_Q(B)$ and $f_Q(B)$ for Bi_2Se_3.

Longitudinal magnon dispersion on the diamond lattice:

$$\hbar\omega_{Q_A} \approx g\mu_B H_0 \pm \sqrt{(8SJf(0) + g\mu_B H_A)^2 - (8SJf(\mathbf{q}))^2},$$

anisotropy exchange

Dilution 3.5%, anisotropy 16 meV, exchange 1 meV.

Kim et al (2013); Zhang et al (2012,2013)

$$\Rightarrow m_Q = [0.12(B_0/2\mathrm{T}) + 0.6]\ \mathrm{meV}$$

Spin wave kinetic term gives:

Li et al (2010);

$$f_Q = 190\ \mathrm{eV}\left(\frac{m_Q(2\ \mathrm{T})}{m_Q(B_0)}\right)^{1/2}$$

Large dielectric constant:

$$\epsilon \sim 100$$

Our mode: high ω, low k → cavity-like resonance w/ L>>1/m_a effective n(B)~0

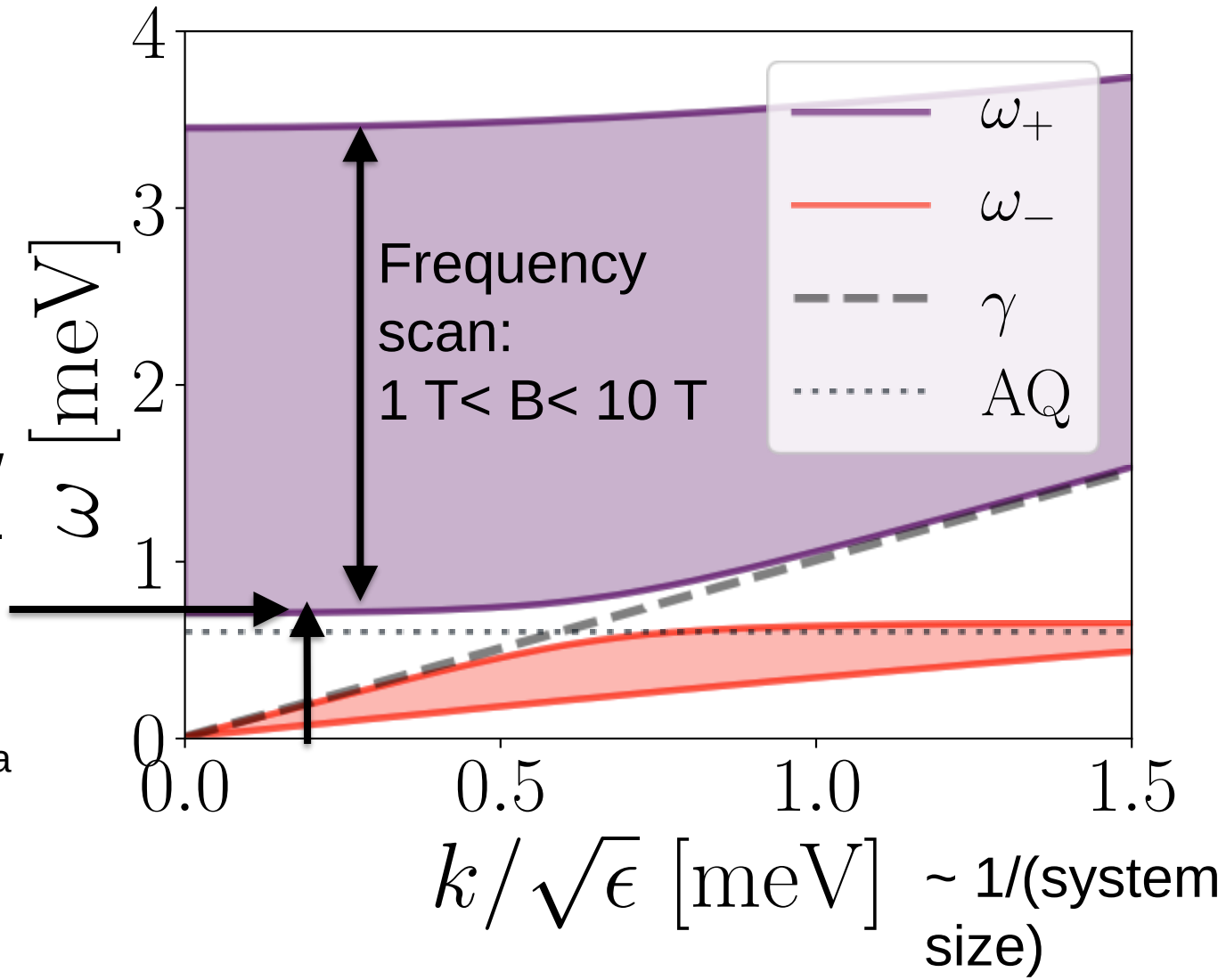

~ 1/(system size)

ϕ_+ polariton has non-zero frequency at k=0, i.e. massive scalar particle.

→ Long wavelength, large volume THz mode for detection.

Detecting small THz signal

$$P_{\mathrm{signal}} = \kappa f_{+} Q_{\mathrm{sys}} P_0$$

coupling, mixing,
resonance

- Following the MADMAX idea, continuity of (D,H) at the dielectric boundary leads to photon emission. Millar et al (2016)
- Losses: $Q=10^5$ (magnetic + emission @100 mK), V=1 cm^3 ➔10^{-22} W at CAST limit: approximately 1 photon per second.
- Photon count vastly improves SNR over radiometer power.
- Dark count rate 0.001 Hz demonstrated at 0.05 K with Quantum Dot Detector (need wide band) Komiyama et al (2000)

Computations & sims ongoing: Millar & Schuete-Engel (MADMAX)

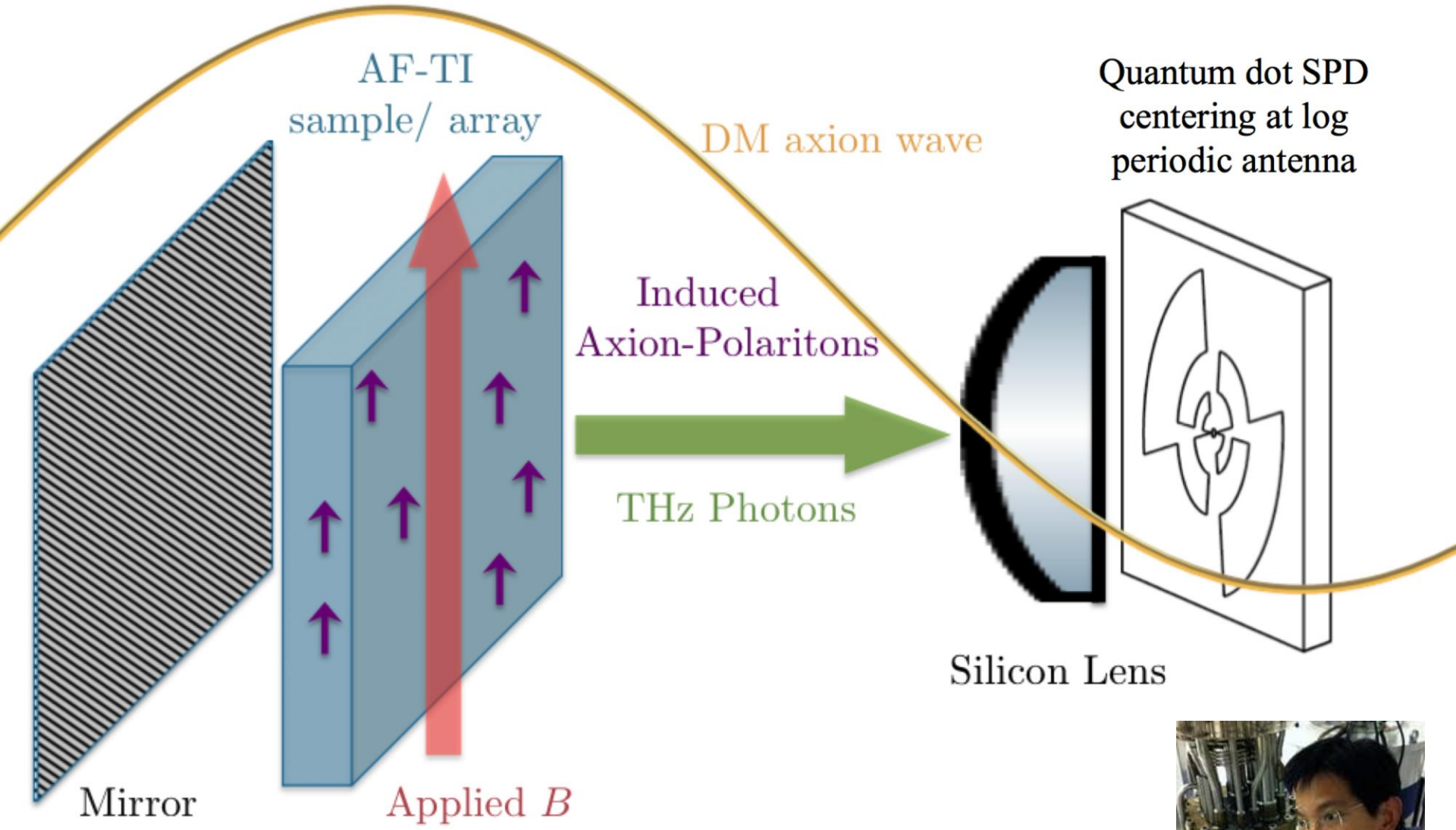
AF-TI
sample/ array
DM axion wave
Quantum dot SPD
centering at log
periodic antenna
Induced
Axion-Polaritons
THz Photons
Silicon Lens
Mirror
Applied B

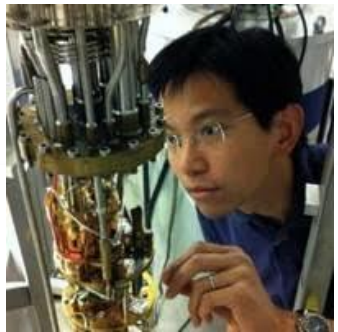

Staged Designs

AF-TI samples limited to ~1 cm^3 for homogeneous doping.
Challenge: increase the effective volume.

Stage I: Single sample, 1cm^3 in thin film.

Stage II: O(100) samples in tiled disk
V_{eff}~100 cm^3.

Stage III: de Broglie limited : V_{effv}~$(0.1\ \lambda_{dB})^3$.

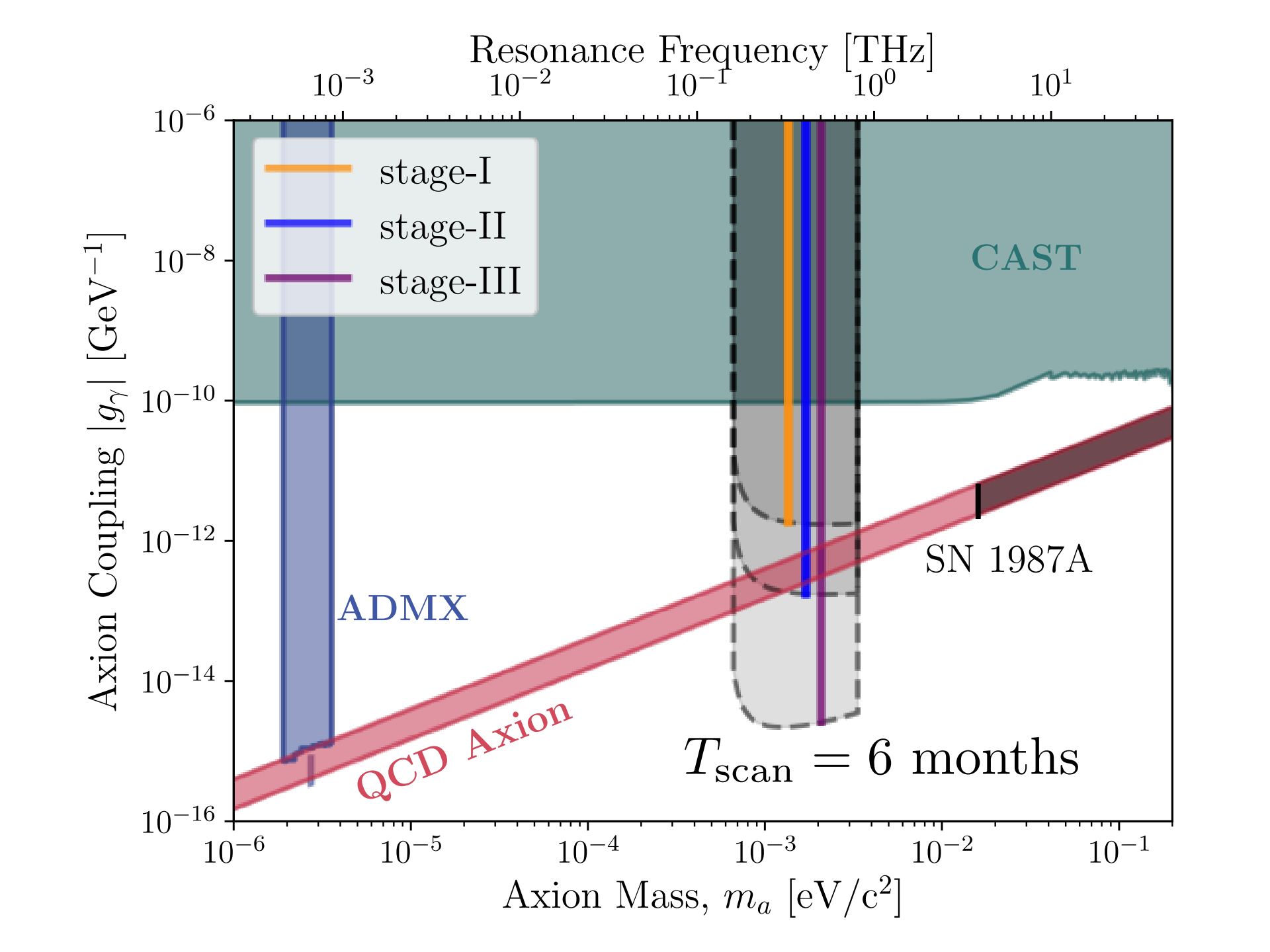
Resonance Frequency [THz]
10^{-3}
10^{-2}
10^{-1}
10^{0}
10^{1}
10^{-6}
10^{-8}
10^{-10}
10^{-12}
10^{-14}
10^{-16}
Axion Coupling $|g_\gamma|$ [GeV^{-1}]
stage-I
stage-II
stage-III
CAST
ADMX
SN 1987A
QCD Axion
$T_{\rm scan} = 6$ months
10^{-6}
10^{-5}
10^{-4}
10^{-3}
10^{-2}
10^{-1}
Axion Mass, m_a [eV/c^2]